communications earth & environment

Article

https://doi.org/10.1038/s43247-024-01251-8

Major changes in fish thermal habitat diversity in Canada's Arctic lakes due to climate change

Daniel P. Gillis [1,2] ✉, Charles K. Minns [1], Steven E. Campana [3] & Brian J. Shuter [1,4]

Climate warming is a major disruptor of fish community structure globally. We use large-scale geospatial analyses of 447,077 Canadian Arctic lakes to predict how climate change would impact lake thermal habitat diversity across the Arctic landscape. Increases in maximum surface temperature (+2.4–6.7 °C), ice-free period (+14–38 days), and thermal stratification presence (+4.2–18.9%) occur under all climate scenarios. Lakes, currently fishless due to deep winter ice, open up; many thermally uniform lakes become thermally diverse. Resilient coldwater habitat supply is predicted; however, thermally diverse lakes shift from providing almost exclusively coldwater habitat to providing substantial coolwater habitat and previously absent warmwater habitat. Across terrestrial ecozones, most lakes exhibit major shifts in thermal habitat. The prevalence of thermally diverse lakes more than doubles, providing refuge for coldwater taxa. Ecozone-specific differences in the distribution of thermally diverse and thermally uniform lakes require different management strategies for adapting fish resource use to climate change.

Ongoing global climate change is drastically altering ecosystems[1]—particularly those in the Arctic[2]—due to the amplification of polar warming through positive cryospheric feedback mechanisms[3]. Lakes integrate atmospheric and catchment-level inputs providing a robust indicator of the impacts of climate change[4]. The remoteness of Arctic lakes ensures that they exhibit the effects of anthropogenic climate change, relatively free from the effects of other anthropogenic stressors[5,6]. Furthermore, lake warming patterns are size-dependent: larger, shallower lakes warm throughout the water column, forming thermally uniform systems; smaller, deeper lakes stratify thermally, with the lower part of the water column remaining cold and isolated from the warmer surface waters, forming thermally diverse systems. Stratification strength is expected to increase with climate warming, particularly for deeper lakes[7]. Lake ice break-ups and freeze-ups are also sensitive to climate conditions, with break-ups generally occurring earlier and freeze-ups later[8,9]. Increases in the ice-free season of two to five weeks are projected by 2050, with deeper lakes experiencing the greatest delays in freeze-up date and northern lakes experiencing the greatest overall impact[9–11]. Increased lake surface water temperatures, extended ice-free seasons, and enhanced thermal stratification with climatic warming will have major impacts on lake water quality, habitat for aquatic biota, and overall ecosystem productivity[12–16].

Arctic freshwater fish communities are dominated by species belonging to the coldwater thermal guild[17]. They are an important ecological, subsistence, and economic resource[18,19], and the effects of climate warming on them will be complex[20]. Climate warming may render some waterbodies less suitable for coldwater fish production[21], while expanding or establishing new thermal resources for coldwater species in lakes that were previously unsuitable[22]. Climate change will also promote the expansion of habitats suitable for coolwater and warmwater fish species with potentially negative effects on coldwater fish production[23]. In thermally diverse communities, coldwater species will face enhanced competition from resident coolwater species, especially in small lakes where spatial resource overlap is high[24]. Expansion of cool and warmwater fish habitats will allow existing coldwater communities to be invaded by species from these guilds, again with likely negative effects on coldwater fish production. Understanding the potential effects of climate change on Arctic freshwater fisheries resources requires a comprehensive assessment of how atmospheric and catchment-level processes affect the thermal dynamics of Arctic lakes and how those changes, in

[1]Department of Ecology and Evolutionary Biology, University of Toronto, 25 Willcocks Street, Toronto, ON M5S 3B2, Canada. [2]Fisheries and Oceans Canada, Species at Risk Program, 200-401 Burrard Street, Vancouver, BC V6C 3S4, Canada. [3]Life and Environmental Science, University of Iceland, Reykjavik, Iceland. [4]Harkness Laboratory of Fisheries Research, Aquatic Research and Monitoring Section, Ontario Ministry of Natural Resources and Forestry, 2140 East Bank Drive, Peterborough, ON K9L 1Z5, Canada. ✉e-mail: daniel.gillis@mail.utoronto.ca

turn, affect the diversity of habitats suitable for different fish thermal guilds. We provide such an assessment in this paper, focusing on (i) predicting the impacts of climate change on the seasonal progression of thermal structure in Canadian Arctic Lakes, and (ii) assessing how those impacts would change the character and diversity of the fish communities present in those lakes. To meet these objectives, we estimated the thermal structure of all Canadian Arctic lakes with surface areas >10 ha ($N = 447,077$). Lake morphometry (maximum and mean depth) was estimated using Geographic Information System (GIS)-based landscape methods and these estimates were ground-truthed using empirical morphometric data from 167 Arctic lakes[13]. We obtained historical (1986–2005) and potential future climate scenarios (Representative Concentration Pathways; RCP4.5 and RCP8.5; 2050 and 2100) to predict seasonal changes in lake thermal structure resulting from projected alterations in local air temperature and wind strength using validated lake temperature, stratification, and ice phenology models[10,25–29] (Figs. 1 and 2, see Methods). Our projections focus particularly on how lake morphometry shapes the impacts of climate change on the diversity of thermal habitats available to support fish from different thermal guilds.

Lakes are projected to increase in temperature, have longer ice-free periods, and undergo thermal stratification more frequently under climate change. Previously inhospitable lakes are expected to no longer freeze to the bottom, thus providing new fish habitat opportunities. Coldwater habitat supply is resilient while thermal refuges for coldwater fish increase in number. In the south, coolwater habitat supply increases and new warmwater habitat emerges, providing invasion opportunities for southerly species. These patterns vary across the landscape, requiring landscape-level variation to be considered in strategies for adapting fish population management to the impacts of a changing climate.

Results

Lake temperature and ice projections

We show historical conditions (1986–2005) and projected future conditions (for 2100 unless noted otherwise, see Supplementary Tables 1–9 for 2050) under two future climate scenarios, representing moderate and high greenhouse gas emissions, respectively (RCP4.5 and RCP8.5). We capture landscape-level variation in impacts by summarizing our results by terrestrial ecozone[30].

Significant lake warming is projected (Fig. 3). Mean-maximum surface water temperature was 14.3 °C (±3.33 standard deviation) for the historical period, with increases of 2.4 °C under RCP4.5 and 2.6 °C under RCP8.5 by 2050. By 2100, increases from the historical mean value reached 2.6 °C under RCP4.5 and 6.6 °C under RCP8.5. The mean ice break-up day of year (183.8) during the historical period shifted 4.9 days earlier under RCP4.5 and 6.4 days earlier under RCP8.5 by 2050. By 2100, the shift from the historical mean value was 6.2 days earlier under RCP4.5 and 12.4 days earlier under RCP8.5. The mean ice freeze-up date (288.6 during the historical period) shifted 8.5 days later under RCP4.5 and 10.7 days later under RCP8.5 by 2050. By 2100, the shift from the historical mean value was 11.2 days later under RCP4.5 and 25.1 days later under RCP8.5. Accordingly, by 2050 the mean ice-free season increased (from a mean of 104.6 days) by 13.5 days under RCP4.5 and 17.2 days under RCP8.5. By 2100, the increase from the historical mean value was 17.6 days under RCP4.5 and 37.7 days under RCP8.5. Projected patterns of change are similar across lake-size classes. The greatest changes are seen in northern ecozones, with ice-free season increases between 17.1 days (RCP4.5) and 20.7 days (RCP8.5) by 2050, and 21.3 days (RCP4.5) and 47.9 days (RCP8.5) by 2100 for the Arctic Cordillera and Northern Arctic ecozones. This is approximately double that of the changes seen in the southwesterly Taiga Cordillera and Boreal Cordillera ecozones, which see increases between 9.7 days (RCP4.5) and 10.4 days (RCP8.5) by 2050 and 12.6 days (RCP4.5) and 23.4 days (RCP8.5) by 2100 (Fig. 4, ecozone mean values from Supplementary Table 1).

Lake thermal habitat projections

We classified lakes as barren, thermally diverse, or thermally uniform for every climate change scenario: (i) barren—winter ice thickness > mean lake depth, fish cannot survive over winter; (ii) thermally diverse—thermally stratified in summer, so that deepwater refuges are provided for coldwater fish; (iii) thermally uniform—thermally mixed in summer, so that warming leads to increased vulnerability to invasion from coolwater and warmwater species. We show how climate change affects: (i) the percentage of barren lakes present in each ecozone (Fig. 5), (ii) the percentage of thermally diverse vs thermally uniform lakes (Fig. 6), and (iii) the relative amount of thermal habitat available for each fish thermal guild in those lakes deemed capable of supporting fish (Fig. 7). We measure thermal habitat in volume-days[17]. This measure includes both the total number of days with suitable thermal habitat and the total volume of suitable thermal habitat. See figure captions and Methods section for methodological details.

The prevalence of thermal stratification increases under climate change. By 2100, thermally stratified lakes increase from 15.8% in the historical period, to 23.8% under RCP4.5 and more than double (+34.7%) under RCP8.5 (Supplementary Table 2). These trends vary by ecozone: in the far north Arctic Cordillera lakes shift from almost 100% mixed lakes

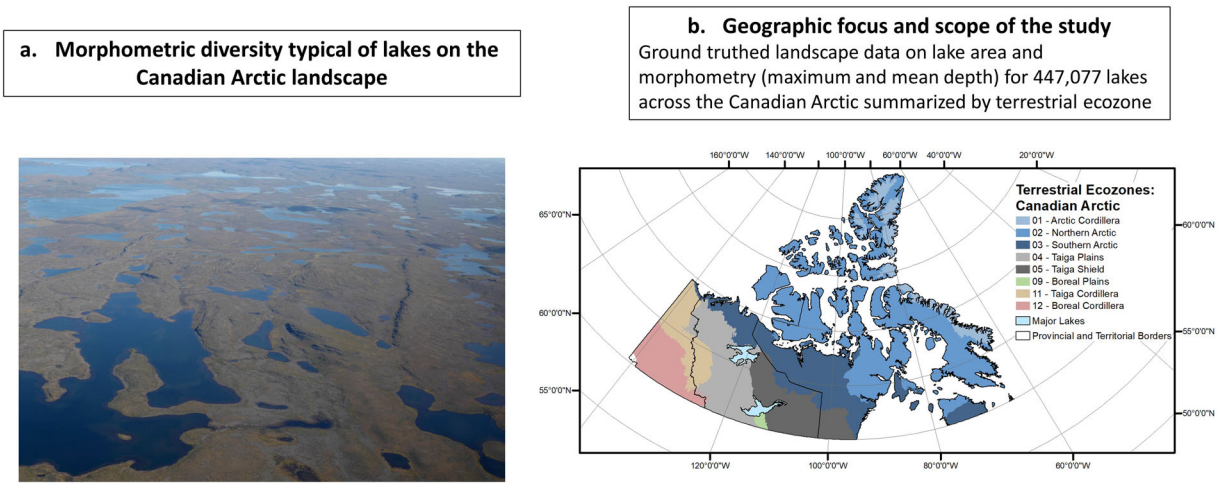

Fig. 1 | The Arctic lake landscape in Canada and its division into terrestrial ecozones. a Aerial photograph illustrating the diversity of lake size and shape common across the Canadian Arctic landscape. **b** The set of terrestrial ecozones used to summarize landscape-level variability in the climate change projections generated in our study plus an overview of the scope of the study.

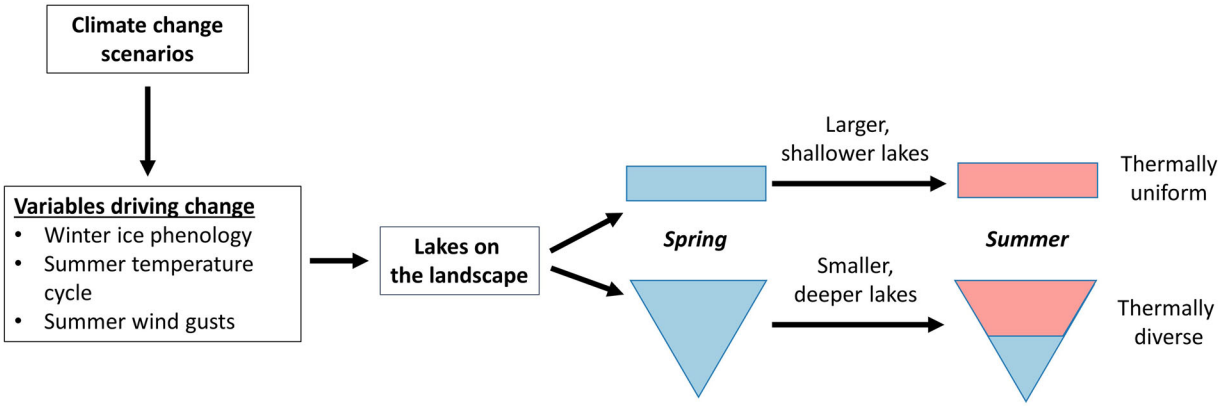

Fig. 2 | Methods used to generate thermal habitat projections. Overview schematic of methods used to generate thermal habitat projections for Canadian Arctic lakes. The shift in thermal structure from spring to summer is shown, with blue indicating a habitat suitable for coldwater fish species and red indicating a warmwater fish habitat. This schematic shows an extreme example, and some lakes may only get warm enough to support coldwater or coolwater fish species in the summer.

under all climate scenarios except RCP8.5 to more than 50% stratified under RCP8.5, while the Boreal Cordillera undergoes a much less drastic shift (Supplementary Table 3).

The barren and thermally uniform lakes decrease, and thermally diverse lakes increase in total number and the total portion of overall lake volume that they comprise under climate change (Figs. 2, 4, and 5; Supplementary Tables 4 and 5). This pattern is driven by thermally uniform lakes becoming thermally diverse (Supplementary Table 6). Barren lakes predominate numerically (Fig. 3), ranging from 52% historically to 45.9% under RCP8.5 2100 (Supplementary Table 4). However, they make up little of the total lake volume due to their shallowness, comprising 5.2% of the total volume historically to 3.9% under RCP8.5 2100 (Supplementary Table 5). Barren lakes are concentrated in the Northern and Southern Arctic ecozones (Fig. 5). Thermally diverse lakes account for the most volume, with 53% of the total volume being accounted by them historically, increasing up to 64.4% by 2100 under RCP8.5 (Supplementary Table 5). Thermally diverse lakes, however, are generally the most scarce numerically (RCP8.5 2100 being the exception at 32.5%, over 21.6% thermally uniform), historically comprising 14.3% of the total lakes and 21.6% of lakes under RCP4.5 2100 (Supplementary Table 4). This difference stems from the fact that thermally diverse lakes are typically deeper than other lakes, hence compensating in volume for what they lack in numbers. Thermally uniform lakes are numerically similar to thermally diverse lakes, ranging from 33.7% historically to 21.6% under RCP8.5 2100 (Supplementary Table 4). They are, however, a smaller portion volumetrically, ranging from 41.7% of total lake volume historically down to 31.7% under RCP8.5 2100 (Supplementary Table 5). Barren lakes that shift status to thermally uniform represent 2.3% (RCP4.5) and 4.9% (RCP8.5) of all lakes in 2100, whereas barren lakes that shift to thermally diverse represent just 0.5% (RCP4.5) and 1.2% (RCP8.5) of all lakes in 2100 (Supplementary Table 6). Thermally uniform lakes that shifted to thermally diverse represent 6.7% (RCP4.5) and 17% (RCP4.5) of all lakes in 2100 (Supplementary Table 6).

The results in the following paragraphs refer to changes by 2100 under RCP4.5 and RCP8.5. Ice-free coldwater thermal habitat in thermally diverse and thermally uniform lakes decreases across climate scenarios, whereas coolwater and warmwater habitat increases. However, trends vary across ecozones (Fig. 7). Ice-free volume-days increase under climate change across ecozones, with the greatest increases being in the far north (e.g., Arctic Cordillera increase in ice-free volume-days of 33.9% (RCP4.5) and 76.5% (RCP8.5), Northern Arctic increase of 24.6% (RCP4.5) and 54.2% (RCP8.5)). The Taiga Shield sees a marked increase in total ice-free volume-days (+22.6% RCP8.5), exhibiting one of the greatest increases in relative coolwater and warmwater thermal habitat. Ice-free volume-days for coldwater fishes decrease from 96.2% of the total ice-free thermal habitat to 84.1% (RCP4.5) and 61.1% (RCP8.5). Coolwater volume-days increases from 3.8% to 15.3% (RCP4.5) and 29.5% (RCP8.5). Warmwater habitat increases from 0% historically to 0.6% (RCP4.5) and 9.4% (RCP8.5) (Supplementary Table 7). The greatest relative decrease in coldwater habitat is projected for the Taiga Shield, which shifts from 90.9% coldwater historically to 35.5% (RCP8.5) (Fig. 7 and Supplementary Table 8). For coolwater habitat, the greatest relative increase is projected for the Southern Arctic, which shifts from 100% coldwater historically to 51.7% coolwater (RCP8.5). Lastly, warmwater habitat saw the greatest relative increase in the Boreal Plains, where it was historically absent and rose to 54.2% (RCP8.5).

Projected longer ice-free seasons under climate change increase the total amount of open-water thermal habitat in Canadian Arctic Lakes, with the supply for each lake type and thermal guild varying greatly across ecozones (Fig. 7 and Supplementary Figs. 1A–D, Supplementary Table 9). Overall, open-water volume-days increased (+14.4% RCP4.5, +30.3% RCP8.5), with coldwater habitat remaining almost at historical levels for RCP4.5 and dropping by 18.9% for RCP8.5. As coldwater habitat drops, we see increases in coolwater and warmwater habitats. Across scenarios, coldwater habitat remains at similar levels for thermally diverse lakes, with reductions in the south roughly balanced by gains in the north; however, there are marked increases overall in coolwater and warmwater habitat—mainly in the Taiga Plains, Taiga Shield, Boreal Plains, and Southern Arctic (coolwater-only)—where they were nearly absent historically (Supplementary Fig. 1C). The coldwater habitat decrease is due to thermally uniform lakes transitioning from coldwater dominant to coolwater dominant in all but the far north (Supplementary Fig. 1D). Coldwater habitat supply predominates and warmwater habitat is low to absent across all lake classifications under all but RCP8.5. Coldwater habitat continues to dominate for thermally diverse lakes, but thermally uniform lakes are comprised of only 45.4% coldwater under RCP8.5, with coolwater nearly taking over at 42.4% (Supplementary Table 9). Furthermore, under RCP8.5, warmwater habitat rises from 0% historically and 0.6% under RCP4.5 to 9.4% of the total (Supplementary Table 7).

Discussion

We assessed the effects of potential future climate change on Arctic lakes and foreseeable effects on fish species of different thermal guilds under two future scenarios. We showed that the proportion of thermally diverse lakes increases under climate change, and coldwater habitat supply is projected to be resilient. Under all climate scenarios, however, thermally diverse lakes shift from providing almost exclusively coldwater habitat to additional coolwater habitat and previously absent warmwater habitat. These changes may make these lakes habitable to larger populations of coolwater species, or invasive warmwater species[31] should they be introduced or naturally expand in these systems through connected waterways. Furthermore, although thermally uniform lakes decrease in prevalence under climate change, they

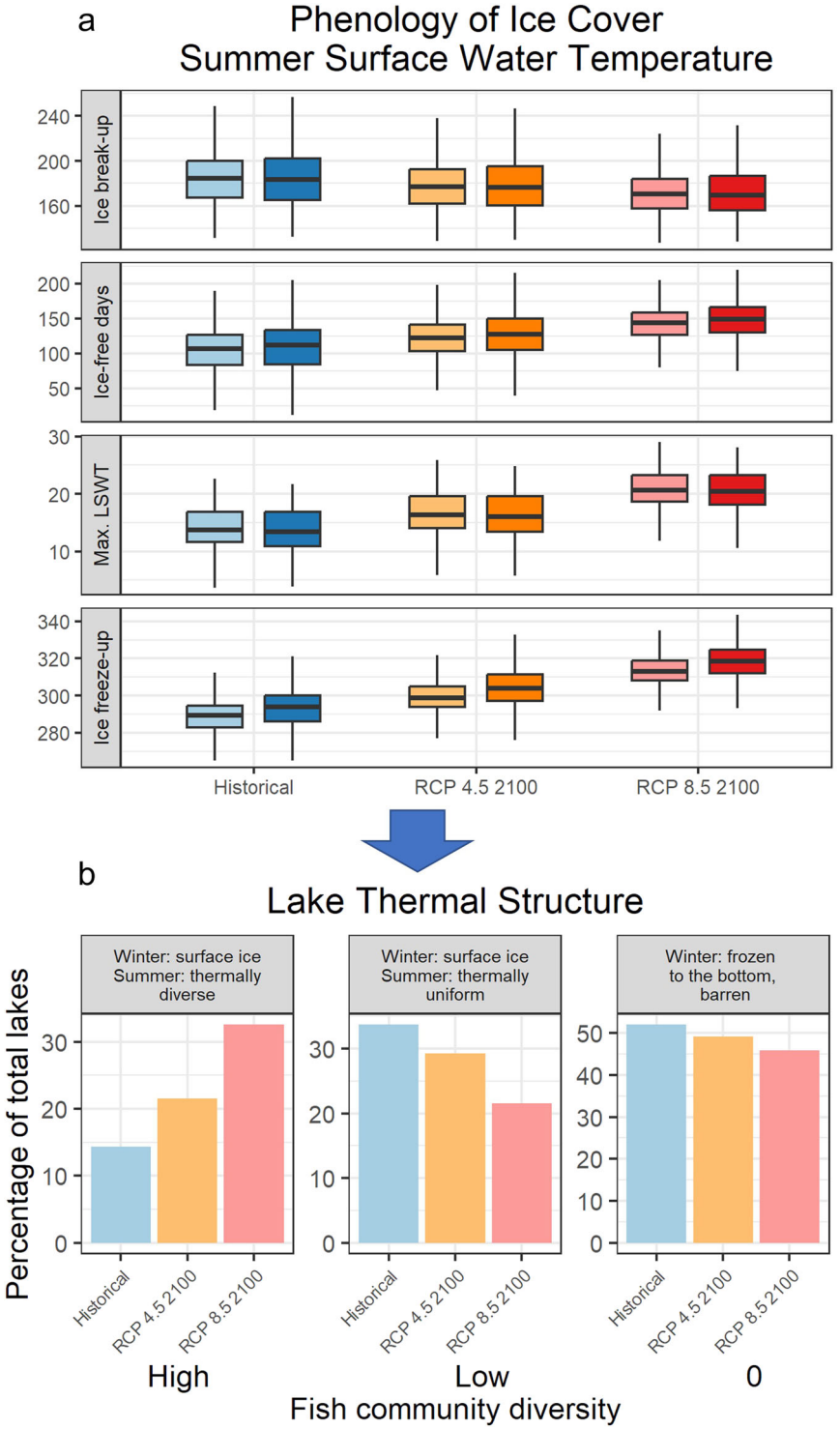

Fig. 3 | Projected maximum surface water temperature and ice dynamics under climate change. **a** Boxplot showing projected maximum surface water temperature (Max. LSWT, °C), ice break-up, ice freeze-up (day of year), and ice-free days (days). Historical and two future potential climate scenarios (RCP4.5 and RCP8.5 in 2100) are shown. Each scenario shows separate results by lake-size class, for small lakes on the left (fetch <5 km, $n = 438{,}587$ (98.1%)) and large lakes on the right (fetch ≥5 km, $n = 8490$ (1.9%)). The box height represents the interquartile range between the 25th and 75th percentiles. The black line inside the box represents the median. The tails on either side of the box represent either the maximum/minimum value in the data, or the 25th/75th percentile plus 1.5 times the interquartile range. Outliers beyond the tails are omitted to accentuate the main trends in the data. Including outliers expands the *y*-axis so that the change in each distribution is visually muted by a few lakes. Furthermore, the modeling system is not designed to simulate extremes (i.e., outliers may be spurious, especially in a large dataset). Across climate scenarios, there is little change in the abundance of barren lakes (decreasing). The greatest shifts occur for thermally diverse lakes (increasing) and then thermally uniform lakes (decreasing). **b** The bar plot shows the climate change impacts on the potential fish community diversity that can be supported by these lakes. The *y*-axis shows the percentage of total lakes represented by that lake class under that climate scenario, and the *x*-axis represents the climate scenario and the fish community diversity that would be supported by thermally diverse (high), thermally uniform (low), or barren lakes (nil).

too will become more favorable to coolwater and warmwater species. Overall, barren lakes decrease in prevalence under climate change as ice thickness lessens, tending to become thermally uniform more often than thermally diverse, which may create opportunities for fish species to colonize and establish in these lakes.

Our projections of Arctic lakes' thermal structure generally align with global lake projections over the 21st century. We projected Arctic lakes to gain 37.7 ice-free days by 2100 under RCP8.5, which is close to the projected average of 40 days for lakes in the Northern Hemisphere by Grant et al.[32]. Our projection of maximum surface water temperature under RCP8.5 was higher (an increase of 6.7 °C) compared to the global average of 4 °C projected by Grant et al.[32], which is consistent with the global trend that ice-covered lakes are warming more rapidly than lakes without seasonal ice-cover[33].

The projected effects of climate change on inland fishes are well-documented and show an unfavorable trend for coldwater species, but most of this work focuses on intensively studied regions south of the Arctic[34,35]. Subsistence fisheries for anadromous Arctic charr (*Salvelinus alpinus*) in Nunavut are important to local communities and their sustainability may hinge on the severity of climate change and changes in community composition through invasive species from the south[36,37]. We show here a much-needed estimate of the historical state of thermal habitat supply in Arctic

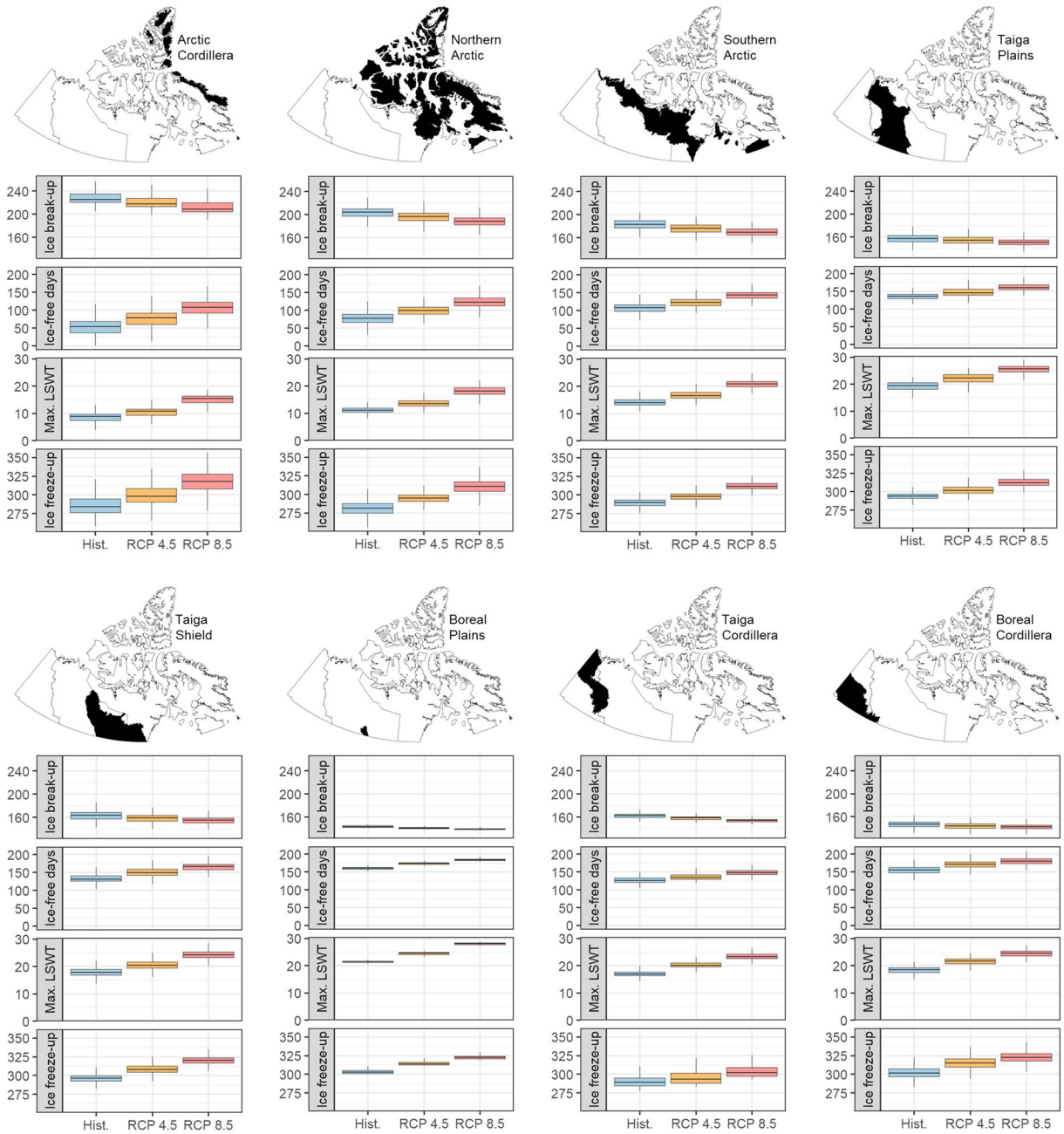

Fig. 4 | Projected maximum lake surface water temperature and ice dynamics under climate change by ecozone. Maximum lake surface water temperature (Max. LSWT, °C), ice break-up, ice freeze-up (day of year), and ice-free days (number of days) projections by ecozone (see Figs. 4 and 5 for *n* lakes per ecozone). Historical and two future potential climate scenarios (RCP4.5 and RCP8.5 in 2100) are shown. The *y*-axes are all set to the global minimum and maximum for each metric across the ecozones. The box height represents the interquartile range between the 25th and 75th percentiles. The black line inside the box represents the median. The tails on either side of the box represent either the maximum/minimum value in the data, or the 25th/75th percentile plus 1.5 times the interquartile range. Outliers beyond the tails are omitted to accentuate the main trends in the data. The shifts to earlier ice break-up dates are minor compared to the shifts to later freeze-up dates. The greatest shifts in freeze-up dates occur in the most northerly ecozones, with approximately 13–31 days being typical in the north compared to approximately 5–20 in the south. Aside from the Arctic Cordillera with modest change, the greatest increases in ice-free days occur in the Arctic Cordillera, Northern Arctic, and Southern Arctic ecozones, with a decreasing trend moving to more southerly/westerly ecozones. A summary of these metrics by ecozone for all five climate scenarios is in Supplementary Table 1.

lakes, providing a reference point for future studies of this much-imperilled region. The limited connectivity of the Arctic hydrological network, however, maintains the diversity of Arctic fishes[38], and thus it is important to consider whether a suitable thermal habitat supply is present even in small lakes, as we have shown here. Fish community productivity in Canada's Arctic lakes is greater than predicted by species-energy theory, highlighting the notion that these habitats may serve as important refugia for coldwater fishes under climate change as their southern range limits become more stressed[39,40].

Policy development and decision-making regarding the protection and conservation of Arctic lakes can be informed by conceptual models weighing the projected effects of climate change—as estimated in our study—and potential future watershed disturbance[41]. With a focus on native coldwater species, true refuge lakes would include lakes projected to be both

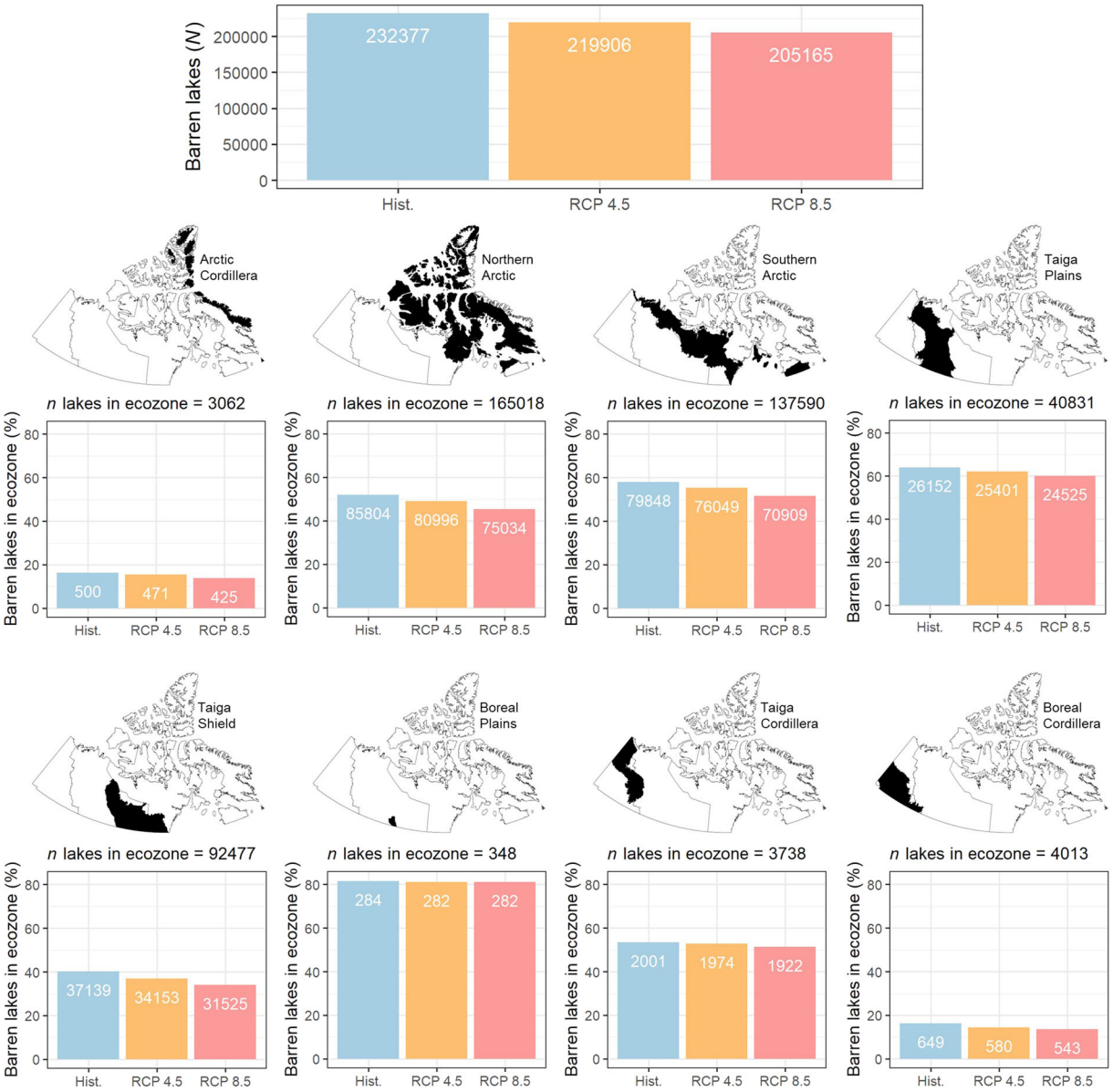

Fig. 5 | Frequency of barren lakes under climate change. Number and percentage of lakes that are classified as barren under historical and two potential future climate change scenarios (RCP4.5 and RCP8.5 in 2100) overall (top) and by ecozone. Changes in the percentages of barren lakes have similar decreasing trends across ecozones but note that barren lakes are concentrated in the Northern and Southern Arctic ecozones. A tally of barren lakes for all five climate scenarios overall (top) is in Supplementary Table 4.

thermally diverse and to retain suitable coldwater habitat supply under climate change[41]. Thermally uniform lakes that retain ample coldwater habitat may be suitable candidates for protection from the kinds of watershed development that would render them unsuitable for coldwater fish[41]. Management actions aimed at protecting coldwater thermal habitat should focus on the above two lake types. Thermally uniform lakes that are unsuitable for coldwater fish under climate change—even with reduced watershed development—may develop into new fish communities of coolwater species, and possibly warmwater species in the most southern lakes[41]. Finite resources for conserving and protecting coldwater fish should be prioritized away from such lakes since such efforts are likely to be unproductive. Informing management decisions with such projections of ecosystem resilience under climate change should ensure the effectiveness of conservation actions aimed at preserving coldwater fish habitat.

Management implications vary because of the differential regional responses to climate change shown here. The projected increase in thermal diversity is greatest in the far north, specifically the Arctic Cordillera and Northern Arctic. The persistence of coldwater habitats, however, suggests that productivity may increase among existing or newly established coldwater fish communities[13] via longer growing seasons and little chance of invasion from distant coolwater and warmwater fish populations[42]. Management implications in the far north therefore would be to explore potential increases in sustainable harvests as conditions change. This possibility becomes muted further south: the Southern Arctic ecozone provides roughly half coolwater and half coldwater habitat under RCP8.5 and hence is vulnerable to coolwater taxa invasions with possibly negative consequences for coldwater fish production[28]. Thermal diversity remains at similar levels under RCP8.5 in the central south ecozones of the Taiga Plains, Taiga Shield, and Boreal Plains; however, the loss of coldwater habitat and increase in coolwater and warmwater is the greatest here. Therefore, the threat to coldwater fish production in these regions is greatest because the opportunities for coldwater fish production offered by higher productivity in warming surface waters is countered by the prospect of those waters becoming too warm for coldwater fish[43]. Waters that become essentially too

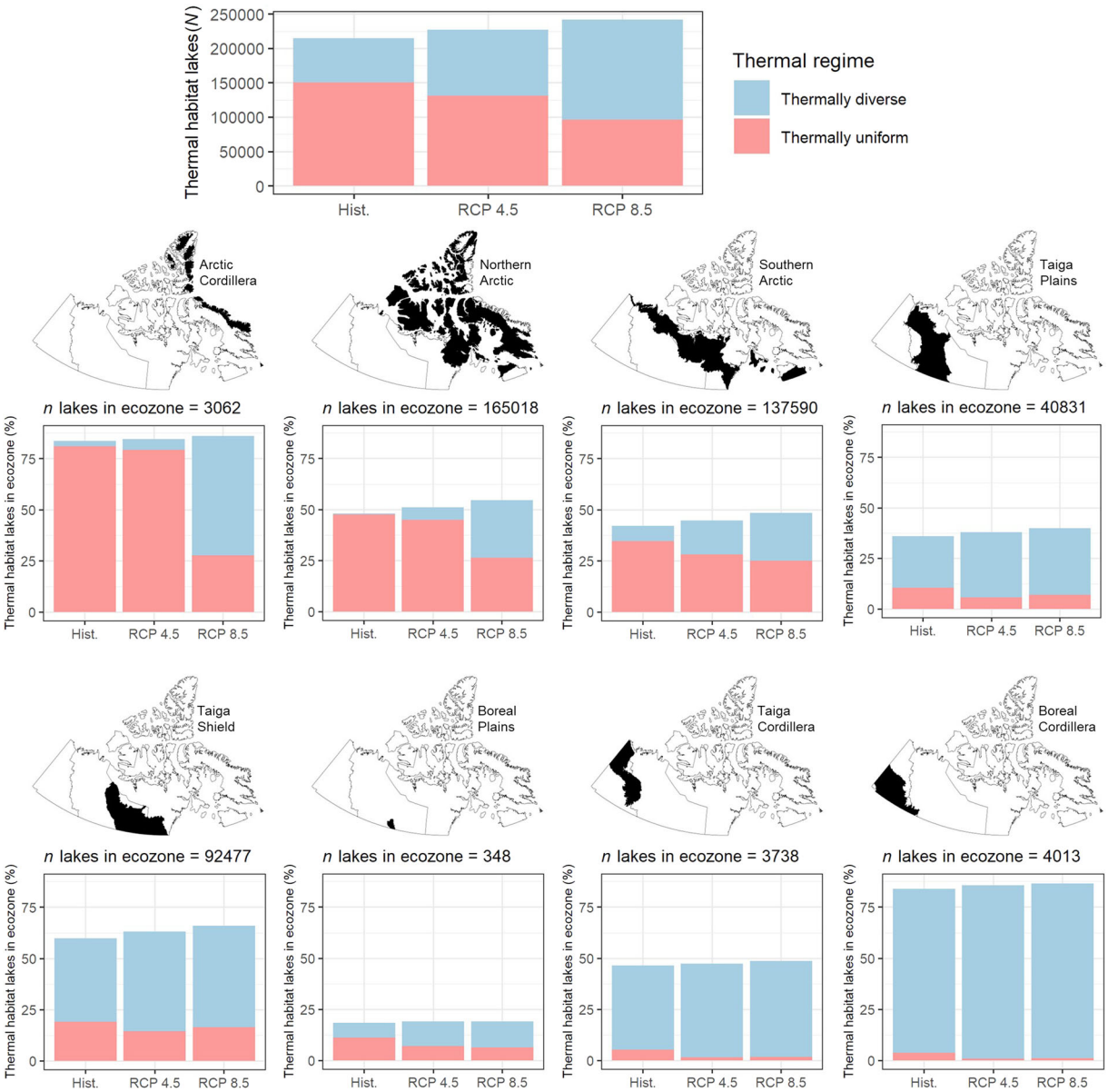

Fig. 6 | Projected lake thermal regimes under climate change. Projected thermal regimes for thermal habitat lakes (i.e., thermally uniform, and thermally diverse lakes, which are included in thermal habitat summaries, with no barren lakes), overall and by ecozone. Historical and two future potential climate scenarios (RCP4.5 and RCP8.5 in 2100) are shown. Barren lakes under each scenario are excluded from these summaries as they are assumed to not support fish. Lakes that transition to thermally uniform or thermally diverse from barren under climate change are included in those scenario's summaries. The *y*-axis represents the percentage of lakes in that thermal regime and plot titles for each ecozone represent the number of lakes. Across ecozones, thermally uniform lakes decrease, and thermally diverse lakes increase in abundance. In the Arctic Cordillera and Northern Arctic, thermally uniform lakes continue to dominate under RCP4.5 but are greatly replaced with thermally diverse lakes under RCP8.5. Thermally diverse lakes typically remain so in the Taiga Shield and Taiga Plains. Historical and two future potential climate scenarios (RCP4.5 and RCP8.5 in 2100) are shown. A tally of thermal habitat lakes for all five climate scenarios overall (top) is in Supplementary Table 4.

warm for use by coldwater fish may permit successful invasion by species belonging to coolwater and warmwater guilds. This possibility is accentuated by the geographical proximity of source populations in the south and the hydrological invasion route offered by the Mackenzie River Basin through the Taiga Plains ecozone[44]. Management implications in these regions should focus on vigilant monitoring and regulation of introductions of coolwater and warmwater fish species. The southwesterly Taiga Cordillera and Boreal Cordillera maintain a high degree of thermal diversity and small though present increases in coolwater and warmwater habitats. In these regions, careful attention and monitoring efforts should be put towards identifying potential establishment points for invaders from the south.

The approach we applied here is intended to provide a first principles accounting of thermal habitat supply in Canadian Arctic lakes under historical and potential future climate scenarios. Using a mix of empirical and process-aligned equations and a simplified view of lake stratification dynamics permits a streamlined approach to this vast and relatively undersampled area. Exploring the application of process-based modeling would allow for a finer exploration of the projected changes in lake's thermal habitat and its drivers. A more detailed approach incorporating temperature variability would be valuable. Our approach used a simple rise and fall in annual open-water lake temperatures, and did not consider the important effects that intra- and inter-annual temperature variation can have on biota[45]. Our results are regionally focused across ecozones, rather than for

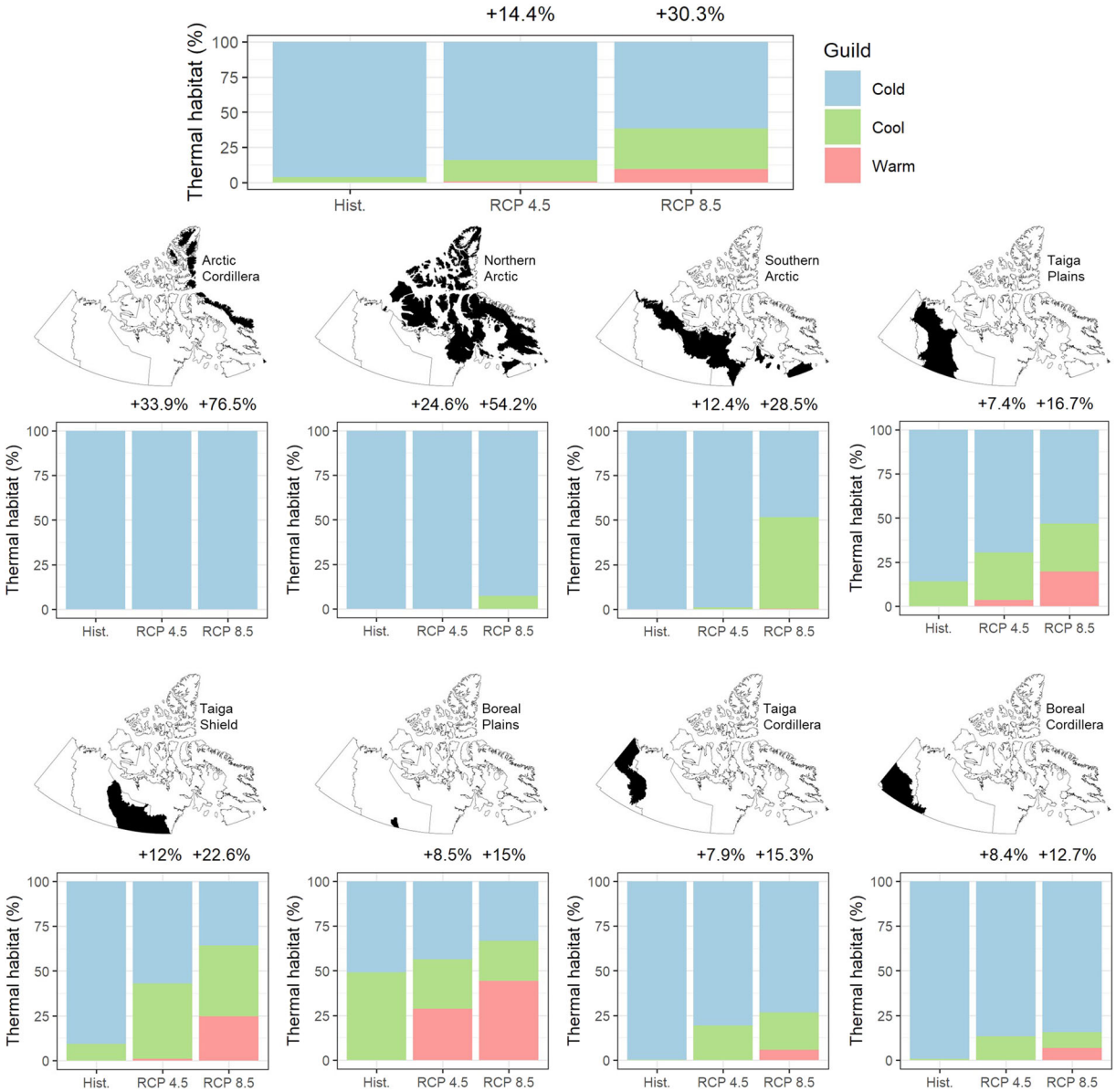

Fig. 7 | Thermal habitat supply across fish thermal guilds under climate change. Ice-free volume-days associated with each thermal guild as a percentage of total ice-free thermal habitat under historical and potential future climate change scenarios (RCP4.5 and RCP8.5 in 2100) for thermally diverse and thermally uniform lakes (barren lakes excluded). The total overall change is shown in the top panel, and by ecozone in the remaining panels (see Figs. 4 and 5 for *n* by ecozone). Great Bear Lake and Great Slave Lake are excluded from volume-days calculations, including the Supplementary Tables. They comprise ~59% of the limnetic volume in the region and as large lakes are subject to complex physical forces, which would skew our results. Barren lakes under each scenario are excluded from these summaries as they are assumed to not support fish. Lakes that transition to thermally uniform or thermally diverse from barren under climate change are included in those scenario's summaries. There are three main groupings of ecozones according to their trends in ice-free volume-days: (1) the Arctic Cordillera, Northern Arctic, and Southern Arctic remain mostly coldwater (except for the Southern Arctic under RCP8.5, which becomes approximately half coolwater), (2) the Taiga Plains, Taiga Shield, and Boreal Plains represent the greatest increases in coolwater and warmwater, and (3) the south-westerly Taiga Cordillera and Boreal Cordillera show small increases coolwater and warmwater. An overall summary (top) of thermal habitat volume-days broken down by lake class and for all five climate scenarios is in Supplementary Table 9.

specific lakes. Although our ground-truthing exercises suggested that the models we employed produce reasonable projections, our methods would not be recommended for focusing on single lakes. We based our thermal habitat boundaries on our definition of thermal guilds. Selecting different thresholds for thermal guilds could alter the interpretation of the results. See the Supplementary Discussion for an extended discussion on these and additional topics for consideration in future research.

Important issues to consider in future assessments of Arctic freshwater fish diversity include: (i) the role of under-ice winter conditions in shaping oxygen deficits and other factors that could limit population establishment and persistence; (ii) changes in the distribution of freshwater across the Arctic landscape due to permafrost melt and subsequent slumping and drainage; (iii) assessing impacts on thermal diversity within the coldwater guild, paying particular attention to species with thermal preferences below 10 °C (the Arctic guild)[46]; (iv) assessing the role of new technologies (e.g., environmental DNA) in designing effective and efficient surveys for monitoring ongoing impacts.

Methods

Overview of the methods used in this paper

The following is an overview of the methods that we used in this paper. Each paragraph has an accompanying sub-section within the Methods section

that provides more details. To develop the approach used in this paper, we applied both empirical and semi-mechanistic methods to build the set of predictive models needed to fulfill our primary objective: (i) predicting the impacts of climate change on the seasonal progression of thermal structure in Canadian Arctic lakes, and (ii) assessing how those impacts would change the character and diversity of the fish communities resident in those lakes[24,35]. A summary of issues addressed, and methods used follows:

(i) Ground-truthing lake morphometry. Lake shape is a primary determinant of lake thermal structure. We used the GIS-based estimates of Canadian Arctic lake morphometry as the basis for our study, hereafter the Arctic GIS lake database[13]. Our Arctic GIS lake database provides the basic information (lake area, mean depth, maximum depth) needed to characterize lake shape[13]. We confirmed the accuracy of those estimates by comparing them to an empirical database of 167 Arctic lakes obtained from a variety of sources (see Ground-Truthing Lake Morphometry section below) with morphometrics directly measured from field surveys.

(ii) Lake-specific predictions of ice-cover phenology and maximum surface water temperature. These are two of the primary elements determining the seasonal pattern of a lake's thermal structure. We mobilized published empirical models to predict the impacts of climate change on these characteristics of Arctic lakes.

(iii) Lake-specific predictions of thermal stratification patterns. Gorham and Boyce[25] developed a semi-mechanistic model linking the character of summer thermal stratification in lakes to the following lake-specific characteristics: the density difference between surface and bottom waters in mid-summer, summer wind strength, and lake fetch. Gillis et al.[27] successfully used this model to predict the presence or absence of seasonal lake thermal stratification. We mobilized various sets of empirical data to ground-truth this model for our set of Arctic lakes. We then used it, along with our other models, to forecast the impacts of climate change on:

- which lakes remain completely frozen through the winter period and hence cannot support a self-sustaining fish community;
- lakes with winter surface ice only. These have the potential to support self-sustaining fish communities and fall into two categories. These are lakes that:
  1. do not stratify during the summer open-water period and hence provide a single, thermally uniform habitat to support their resident fish communities;
  2. stratify into warm surface and cold bottom regions and hence provide a set of thermally diverse habitats to support their resident fish communities.

(iv) Regional predictions of the impact of climate change on stratification patterns in Canadian Arctic lakes. We accessed spatially explicit datasets for historical (1986–2005) climate and projected changes in climate for 2050 and 2100 under RCP4.5 and RCP8.5 emission scenarios using historical and future climate data for each lake from the Government of Canada's climate data extraction tool[29] to generate historical and future climate conditions for each lake in our Arctic GIS database. Using these climate conditions and lake-specific morphometric data as input to the models described above, we estimated historical and future seasonal patterns of thermal structuring for each lake. We then summarized these projected changes across all lakes in each of the eight terrestrial ecozones comprising the Canadian Arctic region[30].

(v) Regional predictions of the impact of climate change on fish habitat diversity in Canadian Arctic lakes. North American limnetic fish species can be classified into three thermal guilds (cold, cool, warm) based on their thermal preferences. We used the historical and projected future patterns of thermal structuring for each lake in our Arctic database to generate annual, lake-specific estimates of the supply (volume-days: m^3 days) of habitat suitable for each thermal guild. We then summarized projected changes in suitable thermal habitat supply across all the lakes found in each of the eight Canadian Arctic terrestrial ecozones.

Historical and future climate data

To drive our limnological projections, we obtained historical (1986–2005) and future (2006–2100) climate data for each lake from the Government of Canada's climate data extraction tool[29]. We assessed the future years of 2050 and 2100 for RCP4.5 and RCP8.5. These RCPs represent greenhouse gas concentration trajectories adopted by the Intergovernmental Panel on Climate Change. Depending on the volume of future greenhouse gas emissions, RCP4.5 and RCP8.5 correspond to the radiative forcing values in 2100 (W m^{-2}). Under RCP4.5, emissions peak around 2040 and then decline, whereas, for RCP8.5, emissions continue rising throughout the 21st century[47]. For simplicity, in our figures, we only show the historical scenario along with RCP4.5 and RCP8.5 for 2100 (omitting 2050), given that under 4.5 the results show similar climates for 2050 and 2100, due to 4.5 stabilizing around the mid-21st century[47].

For mean monthly air temperature data and total monthly precipitation, we accessed the tool's statistically downscaled climate scenario dataset (10 km resolution), based on the Coupled Model Intercomparison Project Phase 5 (CMIP5), which includes 24 climate models with equal model weighting[29]. For mean monthly wind speed, we accessed the tool's Global climate model scenarios dataset (1 × 1° grid resolution), which is also based on CMIP5, and 29 climate models with equal weighting[29]. The climate data extraction tool's map projection is the World Geodesic System 1984 (EPSG:4326).

We estimated hourly global clear sky ground-level solar radiation (W m^{-2}) for each lake according to published procedures and using their recommended air transmission coefficients for every location (elevation data obtained from the ETOPO1 Arc-Minute Global Relief Model[48]), then summarizing the hourly radiation values as monthly means[49]. Next, we used an empirical model to adjust the monthly mean radiation values for location-specific cloud cover[50]. Cloud cover data for the reference period was obtained from the Climatic Research Unit's 0.5 × 0.5° geographic resolution climate dataset[51].

Coordinates of lakes occurring in coastal areas sometimes fell outside the grid cell data range (~0.2% of lakes). For these lakes, we used the mean climate measure for the respective period and climate scenario based on the finest available mean value for lakes in the same National Topographic System grid cell.

Ground-truthing lake morphometry

We assembled a morphometry database of 167 lakes with measured values for surface area, mean depth, and maximum depth. Sources were the Canadian lake surface water temperature database[28], the Fisheries and Oceans Canada Fishout database[39], Canadian Arctic lake trout (*Salvelinus namaycush*) lakes[13], Cumulative Impact Monitoring Program lakes[52], and the Canadian Lakes Assessment Model (CLAM) database[53] (Supplementary Fig. 2). We used these data to assess the accuracy of the morphometry estimates contained within the Arctic GIS lake database. In the Arctic GIS lake database, GIS landscape layers were used to estimate the mean and maximum depth for each lake identified in the landscape layer[13]. This process was done as follows:

- the local land gradients around the edge of each lake were estimated from the Canadian Digital Surface Model and Canadian Digital Elevation Model (http://maps.canada.ca/czs/index-en.html);
- these gradients were extrapolated from the lake edge inward, generating an estimated shape for the lake basin;
- mean and maximum depth for the lake were calculated from this estimated basin shape.

Given that the relationship between mean and maximum depth reflects the basic geometry of a typical lake then, if the algorithms used in generating mean and maximum depth for the Arctic GIS lake database are reliable, we would expect good correspondence between the mean-maximum depth relationship evident in our 167 directly measured Arctic

lakes and the relationship evident in the Arctic GIS lake database. When compared, good correspondence between these two relationships was evident (Supplementary Fig. 3). Since the estimate of basin shape used to estimate mean and maximum depth for the Arctic GIS lake database was derived directly from the local land gradients surrounding the lake, it is reasonable to conclude that validation of the mean-maximum depth relationship is also an indirect validation of the relationships linking lake area to mean depth and maximum depth. Unlike the mean-maximum depth relation, these relationships with lake area are very sensitive to the sampling scheme used to select the lakes for direct measurement. Most lakes in our direct measurement database were chosen because of the known presence of self-sustaining fish populations. Since this requires that lakes be deep enough to not freeze to the bottom over winter, we would expect that, at any given lake area, shallow lakes would be under-represented in our directly measured database. This expectation is confirmed by comparing the one dataset that was compiled without foreknowledge of fish presence (39 lakes in the Cumulative Impact Monitoring Program dataset[52]) with the data in the remaining 128 lakes in the directly measured database (Supplementary Fig. 4).

Given this result, we would expect that the maximum depth-area relationship in the Arctic GIS lake database would exhibit a similar tendency for shallower lakes to be more common at any given depth than is found in the directly measured database and this expectation was met (Supplementary Fig. 5). See the Supplementary Material for an overview of the comparison between the Arctic GIS lake database with HydroLAKES, a widely used global lakes dataset (Supplementary Tables 10–14, Supplementary Figs. 6–9)[54].

Lake-specific predictions of ice-cover phenology

We used empirical lake ice break-up, freeze-up, and thickness models to predict ice-cover phenology[10,55]. The ice models were derived by relating in situ observations of ice phenology and ice thickness for hundreds of Canadian lakes to climate and lake-specific variables through linear regression equations.

The ice break-up model takes the following form:

$$\mathrm{BU} = 175.829 + 1.127 \times J_{\mathrm{SPR0}} - 2.945 \times \mathrm{ANG}_{\mathrm{SPR0}} + 0.0009 \times \mathrm{SA} + 0.491 \times \mathrm{LONG} + 0.017 \times \mathrm{EL} \quad (1)$$

Where:

BU = ice break-up (day of year)
J_{SPR0} = day of the year following the last spring day when the 30-day running mean daily air temperature <0 °C
$\mathrm{ANG}_{\mathrm{SPR0}}$ = angular elevation of the Sun above the horizon at noon on J_{SPR0}
SA = surface area (km^2)
LONG = longitude (decimal degrees)
EL = elevation (m)

The ice freeze-up model takes the following form:

$$\mathrm{FU} = 58.092 + 0.830 \times J_{\mathrm{AUT0}} + 7.293 \times {Z_{\mathrm{MEAN}}}^{0.5} + 0.944 \times T_{\mathrm{AUT0}} \quad (2)$$

Where:

FU = ice freeze-up (day of year)
J_{AUT0} = day of the year following the last fall day when the 30-day running mean daily air temperature >0 °C
Z_{MEAN} = mean depth (m)
T_{AUT0} = mean air temperature for the three-month period where the central month contains J_{AUT0}.

The ice thickness model takes the following form:

$$\ln \mathrm{THK} = -3.968 + 0.801 \times \ln \mathrm{IC} + 1.103 \times \ln \mathrm{LAT} + 0.224/2 \quad (3)$$

Where:

ln THK = the natural logarithm of ice thickness (cm) (reported as m in results to compare with lake depth)
ln IC = the natural logarithm of ice-cover, found by subtracting ice-free days from 365 (ice-free = ice freeze-up − ice break-up) (days)
ln LAT = the natural logarithm of latitude (decimal degrees)
0.224/2 = root-mean-square error from the model used for bias corrections in predictions.

Specific ice thickness values are not central to our results compared to other metrics of thermal structure (e.g., ice-free days, lake temperature), but the general trend is important to determine which lakes are considered to have the potential to host fish populations (i.e., is ice thickness >mean depth?). We compared our projections to published projections for the Northern Hemisphere, with the expectation that our projected decreases in ice thickness would be greater because climate change is expected to particularly impact Arctic ecosystems[2]. We projected lake ice thickness to decrease by 0.22 m (standard deviation = 0.05) on average by 2100 under RCP8.5, which is similar, but slightly higher than the projected average decrease of 0.17 m for the Northern Hemisphere and aligns with our expectation[32].

Lake-specific predictions of maximum surface water temperature

We combined two empirical models in our forecasts of maximum surface water temperature: the T_{MAX} model of Gillis et al.[27] and the SWT model of Sharma et al.[28]. The Gillis et al.[27] T_{MAX} model was based on the assumption that the maximum summer water temperature for a lake could be estimated by:

(i) fitting a triangular function to the spring-fall time series of daily surface water temperatures
(ii) estimating the maximum summer temperature (T_{MAX}) as the peak of the fitted function.

The model's training dataset comprised 240 North American lakes, ranging in latitude from 43–69°N, each providing a year and lake-specific estimate of T_{MAX}[27].

The T_{MAX} model takes the following form:

$$T_{\mathrm{MAX}} = 9.743 - 0.230 \times \ln \mathrm{SA} - 0.0007 \times \mathrm{EL} + 0.996 \times T_{\mathrm{JJA}} - 0.003 \times P_{\mathrm{AUG}} + 0.010 \times \mathrm{CR}_{\mathrm{JUL}} - 0.362 \times W_{\mathrm{JUL}} \quad (4)$$

Where:

ln SA = the natural logarithm of lake surface area (m^2)
EL = elevation (m)
T_{JJA} = mean June, July, and August air temperature (°C)
P_{AUG} = August precipitation (mm)
$\mathrm{CR}_{\mathrm{JUL}}$ = cloud-corrected July solar radiation ($\mathrm{W\ m^{-2}}$)
W_{JUL} = mean July wind speed ($\mathrm{m\ s^{-1}}$)

The Sharma et al.[28] SWT model was based on the assumption that the spring-fall time series of daily surface water temperatures follow a parabolic curve, with the maximum temperature (SWT) occurring at the peak of the parabola. The training dataset used to define this model comprised 2381 North American lakes, ranging in latitude from 42–82°N[28].

The SWT model takes the following form:

$$\mathrm{SWT} = -57.88 + 0.79 \times T_{\mathrm{JUL}} + 0.26 \times T_{\mathrm{ANN}} - 0.00151 \times (J)^2 + 0.617 \times J - 0.019 \times \mathrm{LONG} + \beta \quad (5)$$

Where:

T_{JUL} = mean July air temperature (°C)
T_{ANN} = mean annual air temperature (°C)

J = day of the year when the maximum surface temperature typically occurs, set at 204 for all lakes
LONG = longitude (decimal degrees)
β = a measure of inter-annual variability, set to zero in our study

We compared the projected values for maximum summer surface temperature from these two models across climate scenarios and found that the T_{MAX} estimates were systematically higher than SWT (mean ≈ 3.78 °C, standard deviation ≈ 0.43 °C). This was expected given the difference in how the two methods represent the seasonal time series of surface water temperatures—the triangular function would inevitably yield a higher estimate than the parabolic function. We generated T_{MAX} and SWT estimates for each lake and then used the average of these two estimates in all our subsequent projections.

We did not incorporate in our modeling with the SWT equation any of the mean deviations included for each Canadian territory (and province) in Table 4 of Sharma et al.[28]. We used the base model in that study for all estimates. The mean deviations are broken down by territory and province and do not reflect physical geographic subdivisions (e.g., ecozones). Given that our study is focused on the regional variation in lake thermal habitat changes and that we used ecozone as our geographic classification system, we decided to refrain from incorporating this into our analyses. Future studies could assess the geographic variation of the results that the SWT equation produces on an ecozone level with the goal of producing more accurate predictions of Arctic lake temperatures.

We ground-truthed open-water daily lake surface water temperatures and maximum seasonal surface water temperature with two Arctic Lakes: Alexie Lake (62.68°N, −114.08°W) and Vital Lake (62.61°N, −114.44°W). Data was sourced from Campana et al.[13] and was collected in 2013 over 135 and 122 days for Alexie and Vital, respectively[13]. We also used data from the Toolik Field Station lakes (https://www.uaf.edu/toolik/). These lakes were sampled periodically over several years (1–25 sampling events per year). Lakes that were sampled five or more times in a year were retained following the methods for open-water temperature profile selection used by Gillis et al.[27], resulting in a mean of eight sampling events per year for 11 lakes (96 lake-years). Essentially, we applied a series of temperature value filters to ensure that we were only using temperature profiles measured during the open-water season and not during the ice-covered period of inverse thermal stratification. See Supplementary Figs. 10A–C for an illustration of the lake data and our modeling results.

For Alexie Lake, root mean squared error (RMSE) and correlation (r) between predicted and observed surface water temperatures were most favorable for T_{MEAN} (the average of T_{MAX} and SWT: RMSE = 2.17 °C; $r = 0.887$, $p < 0.0001$, $n = 134$). For Vital Lake, the SWT model produced the most favorable results (RMSE = 2.09 °C; $r = 0.868$, $p < 0.0001$, $n = 122$), but the RMSE for T_{MEAN} was only 0.06 °C higher than the SWT value. The Toolik lakes had the lowest RMSE for the averaged value (RMSE = 2.56 °C) and the highest correlation under T_{MAX} ($r = 0.617$, $p < 0.0001$, $n = 770$), though the T_{MEAN} correlation was only 0.007 lower than the T_{MAX} value.

Maximum lake surface water temperature was predicted best by T_{MAX} for Alexie and Vital, and by T_{MEAN} for the Toolik lakes in terms of RMSE. The observed maximum lake surface water temperature for Alexie was 22.0 °C. T_{MAX} predicted a value of 23.1 °C (+ 1.1 °C observed), SWT predicted 18.1 °C (−3.9 °C observed), and thus T_{MEAN} was 20.6 °C (−1.4 °C observed). The observed maximum lake surface water temperature for Vital was 22.8 °C. T_{MAX} predicted a value of 23.5 °C (+ 0.7 °C observed), SWT predicted 18.1 °C (−4.7 °C observed), and thus T_{MEAN} was 20.8 °C (−2.0 °C observed). For the Toolik lakes, RMSE between predicted and observed maximum lake surface water temperature was 1.66 °C for T_{MAX}, 2.10 °C for SWT, and 1.55 °C for T_{MEAN}. The average observed value was 16.0 °C. T_{MAX} overestimated with an average of 16.7 °C, SWT underestimated with an average of 14.6 °C, and T_{MEAN} underestimated with the closest value of 15.6 °C. The correlation was greatest for T_{MAX} ($r = 0.504$, $p < 0.0001$, $n = 96$), followed by T_{MEAN} ($r = 0.499$, $p < 0.0001$, $n = 96$) and then SWT ($r = 0.449$, $p < 0.0001$, $n = 96$). It is of note that the Toolik lakes were not sampled daily like Alexie and Vital, so it is unlikely that the actual maximum temperature was captured in the observed data, as the average lake was visited eight days throughout the open-water season.

Overall, our results indicate that each modeling approach has its merits for different lakes, and balancing the outputs using average values yields similar or improved accuracy in many cases. It is not surprising that the T_{MAX} overestimated the maximum temperature and SWT underestimated it as the T_{MAX} model produces a linear seasonal rise and fall, whereas SWT produced a parabolic curve. Overall, these results are in line with the results obtained in the studies that developed these models as well as other studies that generated lake temperature predictions across a large landscape[27,28,56,57]. These results suggest that the modeling approach we employed produces reasonable estimates for the purposes of our study. Future research could investigate the potential for additional model testing and refinement with the use of additional high-resolution monitoring data.

Lake-specific predictions of stratification and thermocline depth using the Gorham-Boyce approach

Gorham and Boyce[25] present a simple semi-mechanistic model that links climatological variables with the physical theory of mixed layer formation to predict, for a particular lake:

- if the lake stratifies or not
- if the lake does stratify, its thermocline depth (h)

Their model is based on the following equations:

$$H \cong 3.4\left(\frac{\tau}{g\triangle\rho}\right)^{0.5} L^{0.5} \quad (6)$$

and

$$h = \frac{H}{1.7} \quad (7)$$

Where:
h = lake thermocline depth
τ = wind stress associated with summer storms (i.e., stress associated with the maximum sustained wind strength likely to be experienced by the lake during summer)
$\Delta\rho$ = density difference between epilimnion and hypolimnion at the time of maximum heat content
L = maximum lake length
g = gravitational acceleration
H = critical mixing depth

If the lake's maximum depth is ≤H, then it will not stratify. If the lake's maximum depth >H, then it will stratify with a thermocline depth = h. These equations identify the contending climatic forces that determine the pattern of stratification in a lake of given morphometry (i.e., fixed L): through τ, higher winds drive both the critical mixing depth and consequent thermocline depth deeper; through $\Delta\rho$, higher summer temperatures drive the critical mixing depth, and consequent thermocline depth, shallower. The Gorham-Boyce approach is flexible and has recently been applied to describe a novel thermal categorization of ice-covered lakes[58].

The Gorham-Boyce approach applies to lakes with a cross-basin diameter <5000 m. The Arctic GIS lake database comprises 98% of lakes with maximum length values <5000 m. We set the upper limit of thermocline depth at 20 m based on previous studies, which show that the impact of lake length on thermocline depth is limited when lake length exceeds 5000 m[25,59].

A detailed description of how we implemented the Gorham-Boyce approach is provided in the following paragraphs. Here we focus on the results of ground-truthing tests we conducted to assess the reliability of our implementation of this approach. We began by using observed thermal stratification data from Alexie Lake and Vital Lake. These lakes were

described and used to ground-truth the methods described in the section titled Lake-specific predictions of maximum surface water temperature[13]. We used the R package 'rLakeAnalyzer' to calculate the daily thermocline depth using the *ts.thermo.depth* function. We then used the *approx.bathy* function to divide the total lake volume into successive 1 m layers. Using the *internal.energy* function, we calculated the daily heat content for each layer, and summed these values across the water column to obtain the daily lake heat content. Lastly, we filtered the thermocline depth time series for the date of maximum heat content and used the empirical values for each lake as a reference point for the Gorham-Boyce approach (Vital observed $h = 5.7$ m, Alexie observed $h = 7.6$ m). The Gorham-Boyce equation produced an estimated thermocline depth at maximum heat content (h) of 6.6 m for Vital (+0.9 m observed) and an h of 7.8 m for Alexie (+0.2 m observed). These results indicate that the Gorham-Boyce equation produces a reasonable estimate of thermocline depth in these two stratified lakes (Supplementary Fig. 10C). We also tested the Gorham-Boyce approach with the Toolik lakes (described and also used in the section titled Lake-specific predictions of maximum surface water temperature). The same methods were used to obtain the observed thermocline depth on the date of maximum heat content. One observation was omitted (lake NE14, year 2009) because the observed thermocline depth on the date of maximum heat content was much deeper than in the other two years it was measured (2009 = 13.9 m, 2010 = 4.5 m, 2011 = 6.9 m). This resulted in 95 lake-years to analyze. As noted for the lake temperature model testing, the Toolik lakes were not sampled daily and had an average of eight visits per year, so it is unlikely that the actual thermocline depth at maximum heat content was accurately captured by the sampling events. For the Toolik lakes, stratification presence was predicted with 84.6% accuracy, with 77 out of 91 lake-years observed to stratify being correctly predicted (84.9% accuracy when including Alexie and Vital). One lake (lake E6, maximum depth 3 m) comprised 13 of the 14 incorrect stratification presence predictions. Lake E6 stratified 13 out of the 16 years it was sampled, and the Gorham-Boyce equation predicted it to be mixed for every year. Hence, it correctly predicted mixing in only three out of the sixteen years. The equation's output suggested that with all other equation variables held equal, E6 would need to be between ~4.5–5.9 m deep to be predicted as stratified by the Gorham-Boyce method. The other incorrect prediction was for lake S7 (maximum depth 3.3), which was sampled for two years. In one year, it was correctly predicted as mixed, and in the other, it was incorrectly predicted as mixed because it was observed as stratified. The equation's output suggested that S7 would need to be 3.33 m deep to be classified as stratified, so the equation was very close to predicting the correct thermal state. The following results are for the 77 Toolik lake-years where stratification presence was accurately predicted, as well as for Alexie and Vital lakes. The correlation between observed and predicted thermocline depth across all Toolik lakes was highly significant ($r = 0.573$, $p < 0.0001$, $n = 77$), and increased slightly with the addition of Alexie and Vital ($r = 0.579$, $p < 0.0001$, $n = 79$). The RMSE was 1.96 m for the Toolik lakes and 1.93 m when Alexie and Vital were added. The mean observed thermocline depth across all Toolik lake-years was 4.89 m, compared to the mean predicted depth of 4.80 m (4.93 m observed average and 4.86 m predicted average with Alexie and Vital). These results indicate that the Gorham-Boyce equation produces a reasonable estimate of thermocline depth for lakes that stratify, and a reasonable level of predictive accuracy for whether a lake is mixed or stratified (Supplementary Fig. 10C).

These equations also require that, among lakes that stratify at a given fetch, the maximum depth will be ≥1.7 × thermocline depth. We submitted this expectation to an empirical test as described below.

Hanna[60] provides the most extensive empirical description of the relationship between lake fetch and thermocline depth. The equation produced by Hanna[60] takes the following form:

$$\ln h = 0.336 \times \ln \mathrm{MEL} - 0.245 \quad (8)$$

Where:

ln h = the natural logarithm of lake thermocline depth (m)

ln MEL = the natural logarithm of maximum effective lake length, taken as maximum lake length (L) in our study (m)

The red crosses in Supplementary Fig. 11 are the Hanna relationship multiplied by 1.7 and the blue dots provide the maximum depth-fetch relationship for lakes that consistently stratify (152 lakes in the first figure of Gorham and Boyce)[25]. If the maximum depth is ≥1.7 × thermocline depth (as required by the Gorham-Boyce equations) then the crosses should define a clean lower bound for the maximum depth data and Supplementary Fig. 11 confirms this expectation. This result provides additional support for our use of the Gorham-Boyce semi-mechanistic structure as the foundation for our projections. In what follows, we will refer to this bounding relationship (as defined by applying the Gorham-Boyce equations to Hanna's empirical result) as the Hanna Line.

The Gorham-Boyce equations identify the lake-specific elements needed to predict h and H:

- the water density difference between epilimnetic and hypolimnetic waters at the time of maximum heat content,
- the summer wind regime,
- lake fetch.

The following paragraphs describe in detail how we implement these equations in our climate change projections.

We developed an approach to predict the density difference between the epilimnion and hypolimnion. The first table in Gorham and Boyce[25] (hereafter GBT1) summarizes data on the temperature difference between epilimnion and hypolimnion at the time of maximum heat content for 166 lakes that consistently stratify. These lakes are in North America ($n = 109$), Europe ($n = 23$), and Japan ($n = 34$). Individual values in the table represent values for a single lake, with some lakes identified specifically by name. Where there are many lakes located in a relatively restricted geographic area, values for the smallest and largest (by area) lakes are provided. These lakes are not named specifically. The group in GBT1 labeled mid-NA contains 67 lakes, but some of the lakes in the other groups are included in this group, specifically the Laurentian Great Lakes. However, the smallest lake (surface area = 1.7 ha) is not part of any of the other groups. We used the data in this table to develop a simple regression model for predicting the hypolimnetic and epilimnetic density difference typical of lakes that consistently stratify. There were 22 individual lakes (omitting the Laurentian Great Lakes) identifiable in GBT1, ranging in area from 0.4–64,770 ha (median = 289 ha). We chose these lakes for our analysis of the drivers of the hypolimnetic-epilimnetic density difference. We omitted the Laurentian Great Lakes because of the huge discrepancy in area and volume between these systems and all the other lakes in GBT1. We converted the temperature differences recorded in GBT1 to density differences. We used multiple regression analysis, filtering results using the Akaike information criterion, to arrive at the following usable (adjusted $R^2 = 0.95$, $n = 22$) model for predicting, from known lake variables, the difference in density between hypolimnetic (HYPO) and epilimnetic (EPI) waters at the time of maximum heat content for stratified lakes:

$$[\mathrm{HYPO} - \mathrm{EPI}] = -2.11264 + 0.20607 \times T_{\mathrm{EPI}} - 0.00487 \times [T_{\mathrm{EPI}} \times \log_{10} L] \quad (9)$$

Where:

[HYPO – EPI] = the density difference at the time of maximum lake heat content (g cm^{-3})

T_{EPI} = epilimnetic temperature (°C) at the time of maximum lake heat content

$\log_{10} L = \log_{10}$ lake maximum length, or fetch (m)

In using this model for predicting the density differences for the lakes in the Arctic GIS lake database, we set T_{EPI} = the mean of the T_{MAX} and SWT models for maximum surface water temperature. In addition, we used these

estimates of maximum surface temperature and density difference to estimate the hypolimnetic temperature.

We predicted summer storm intensity to apply the Gorham-Boyce approach to our study area. With both lake fetch and density difference given, the Gorham-Boyce equations predict that H will increase with increases in the wind strength of typical summer storms. An overall increase in H will be accompanied by a drop in the % of lakes in a region that will stratify, and a parallel increase in the thermocline depths (h) of those lakes that still stratify. Our approach to characterizing the strength of summer windstorms proceeded in several steps:

(i) we characterized the historical pattern of summer wind strength variation, typical of our Arctic study area;
(ii) we defined a representative sample of our 447,077 Arctic lakes, containing ~2% (9623 lakes) of the total;
(iii) we used this representative sample of Arctic lakes and the historical pattern of Arctic wind strength variation to determine if there was a typical value for the strength of a summer windstorm that would position the distribution of maximum depth for stratified lakes so that it is was bounded below by the Hanna Line, as illustrated in Supplementary Fig. 11.

We used historical patterns of summer wind strength variation in the Canadian Arctic to characterize a pattern of wind strength variation typical for this landscape. We selected a representative set of Arctic locations as follows:

- for lakes in the Arctic GIS lake database north of 60°N latitude, we calculated the 25th, 50th, and 75th percentiles of latitudes (63.23, 65.82, and 68.38°N) and longitudes (−113.69, −104.25, and −93.01°W);
- we used these points to define a rectangular grid made of nine representative locations that we confirmed were located on land;
- we then identified 12 sites in the neighborhood of each of these 9 representative locations and used the Government of Canada's Wind Atlas climate tool (www.windatlas.ca) to derive summer wind speed distributions for each of these locations.

The Government of Canada's Wind Atlas climate tool (www.windatlas.ca) gives wind speeds at 10-minute intervals (at 80 m height) throughout June, July, and August; the speeds given are for the years 2008–2010. We adjusted the wind speed at 80 m height to 10 m (the value required for the lake thermal habitat modeling, e.g., Wuest and Lorke[61]) using the formula provided by Hsu et al.[62]:

$$U_{10} = U_z\left(\frac{10}{z}\right)^{0.11} \quad (10)$$

where U_z equals the wind measured at height z above the lake's surface.

We analyzed mean wind speeds at three-time scales (1, 8, and 24 hours) by fitting a Weibull distribution (see Conradsen et al.[63] for the relevance of the Weibull distribution as a descriptor of variation in wind strength) to the vector of summer wind speeds (June, July, August) for each site for the 3 summers (2008 to 2010) provided by the Wind Atlas. Summarizing across locations, we found that the value of the Weibull shape parameter (β) increased with time scale (Supplementary Table 15) but that there was no systematic variation with either latitude or longitude. We assumed that:

- the 1-hour wind speed distribution was the most relevant for estimating H;
- the median value for the 1-hour shape parameter ($\beta = 2.338$) was a reasonable approximation of this parameter for all sites;
- this parameter would be insensitive to changes in climate.

With β fixed, the scale parameter (η) of the Weibull distribution can be easily estimated if the mean wind speed is known. Mean wind speeds are provided in the projections of historical and future climatic conditions that we use in this study[29], so we were able to use these projected mean values and our fixed value for β to estimate future changes in the Weibull distribution for summer wind strength values.

We defined a manageable sample of our 447,077 lakes that we could use in a series of simulations designed to determine if there was a single summer windstorm strength measure that would replicate the bounding relationship in Supplementary Fig. 11 for lakes that the Gorham-Boyce model predicts would stratify. We set our sample size at 2% (9623 lakes) of the total number of lakes ($N = 481{,}784$) in the original Arctic GIS lake database[13]. Approximately 7% of the sample contained lakes with latitudes south of 60°N latitude ($n = 690$ lakes, °N range = 51.913–59.999, mean °N = 65.39). We believe that the inclusion of these lakes does not drastically impact our results as the average latitude of the Arctic GIS lake database with only lakes at least 60°N is 65.95°N, which is only approximately 0.56° latitude different, or about 62 km, which is negligible considering the vast scale of our study area. We believe that this sample size is large enough to be representative yet still small enough to allow for logistically feasible simulation times. The original Arctic GIS lake database was sampled and we used the *slice_sample* function from the R package 'dplyr', parameterized to ensure that the resultant sub-sample of lakes was representative of each ecozone and lake-size class in the entire database[64]. We then used this sub-sample of lakes to simulate how increases in summer wind strength affect the distribution of maximum depth among stratified lakes, given the Gorham-Boyce equations and lake-specific values for:

- fetch,
- epilimnetic and hypolimnetic density difference,
- the location-specific Weibull distribution for summer 1-hour wind strength.

Given the historical value for mean summer wind speed for each lake, we conducted successive simulations at progressively higher levels for storm wind speed until we identified a level that would replicate, in our sample of 9623 lakes, the bounding relationship in Supplementary Fig. 11 for lakes that consistently stratify. We assumed that the local temporal variation in 1-hour summer wind speed was described by a Weibull distribution defined by the local mean wind speed and the shape parameter ($\beta = 2.338$) that we determined (see section above) to be typical of sites in our study area. We defined summer storm wind speed as that defined by a fixed percentile value for the cumulative distribution (CD) of this local Weibull function. The same percentile value was applied to all lakes in a particular simulation and each simulation was then characterized by a progressively higher value for this fixed CD percentile. We used this procedure to identify the single percentile value that positioned the simulated maximum depth distribution for stratified lakes so that it was bounded below the Hanna Line, as illustrated in Supplementary Fig. 11. We used the following formal bounding procedure to do this:

(i) for each simulation, we used quantile regression to estimate the relationship between the first quartile of the maximum depth distribution of stratified lakes and fetch;
(ii) we compare this relationship with the maximum depth/fetch relationship defined by the Hanna Line;
(iii) we declared bounding as successful when the two relationships overlapped.

We found that a match with the Hanna Line was obtained with the CD percentile = 99.9999 (Supplementary Fig. 11). These assumptions have wide implications for the following analyses, and future work could explore other relationships that may further validate the values used in similar analyses.

A detailed description of this fitting procedure for historical climatic conditions follows. For each lake in a simulation:

1. given the fetch and location of the lake, the relevant climate variables were extracted from the historical climate database;
2. the summer maximum temperature and consequent value for the density difference ($\Delta\rho$) were estimated using the empirical models described in previous sections;

3. the local variation in 1-hour mean wind strength ($m\,s^{-1}$) was represented as a Weibull function, with the shape parameter set at the value ($\beta = 2.338$) we determined to be representative of our study area and scale parameter (η) consistent with the local mean wind speed given in the historical climate database;
4. the typical strength of summer windstorms was set at the value specified by the simulation-specific trial value for the CD percentile for this Weibull function;
5. this value for storm wind strength at 10 m above the lake surface (U_{10}) was included in the following formula for wind stress (τ):

$$\tau \equiv \rho_w u_*^2 = \rho_a C_{D,10}\left(U_{10}^2\right) \quad (11)$$

where ρ_w is water density (set to 1000 $kg\,m^{-3}$ here), ρ_a is air density (set to 1 $kg\,m^{-3}$ here), and $C_{D,10}$ is the drag coefficient for surface winds at 10 m[25];

6. we calculated the drag coefficient using Charnock's Law[65] and an empirical relationship[61]:

$$C_{D,10} = \begin{cases} 0.0044 \times U_{10}^{-1.15}, U_{10} < 5m\,s^{-1} \\ \left[k^{-1}\ln\left(\frac{10g}{C_{D,10}U_{10}^2}\right) + 1.13\right]^{-2}, U_{10} > 5m\,s^{-1} \end{cases} \quad (12)$$

where k is the von Karman constant (0.40), and g is the gravitational acceleration;

7. the resultant values for τ and $\triangle\rho$ were then included in the Gorham-Boyce equation for the critical mixing depth (H);
8. if this estimate for $H >$ maximum depth for the lake, the lake was designated as thermally uniform throughout the open-water period;
9. if this estimate for $H \leq$ maximum depth for the lake, the lake was designated as thermally diverse, with the difference in temperature in mid-summer equal to the epilimnetic-hypolimnetic temperature difference;
10. in the case of some far north lakes, the estimate for maximum surface water temperature was less than the estimated hypolimnetic temperature—in these cases, we designated the lake as thermally uniform;
11. in addition, an upper bound of 20 m for thermocline depth was set based on studies on the Laurentian Great Lakes[25,66].

Once the stratification state for all 9623 lakes was determined using this procedure, we fit a first quartile regression to the distribution of maximum depth values for stratified lakes, with $\log_{10}$ fetch (km) as the independent variable and $\log_{10}$ maximum depth (m) as the dependent variable. We then compared this regression line to the Hanna Line. We carried out a series of these simulations, each one characterized by a progressively higher value for the Weibull CD percentile used to characterize summer storm wind strength. We found the 99.9999 percentile met this fitting criterion (Supplementary Fig. 11) with 14.6% of the lakes in the sample predicted to stratify under historical climate conditions.

Our use of local wind conditions in the Arctic was predicated on the notion that these would include some degree of the local terrain characteristics, which is mainly a treeless landscape. Southerly lakes would have wind sheltering from trees. Although the models that were developed and tested in these locations should be widely applicable in principle, they may require special considerations for Arctic systems that we did not fully test. The above tests were grounded in the notion that the Gorham-Boyce model and Hanna Line were based on a wide-ranging array of lakes that were accessible to detailed monitoring programs[25,60]. It is worth noting that although these datasets did not include any lakes north of 60°N, they did contain latitude ranges of 31–54°N (Gorham-Boyce) and 32–55°N (Hanna), along with elevation ranges of 10–3900 m (Gorham-Boyce) and 10–1897 m (Hanna)[25,60], showing that the datasets did reach latitudes close to the Arctic Circle and high elevation lakes. Future research may consider how the environmental context of the Arctic may dictate lake thermal dynamics in ways that differ from temperate regions. Model testing and development would be warranted in this pursuit. Overall, Arctic lakes may be mixed more often than expected due to the lack of buffering from vegetation. We also address this in part by using fetch as our measure of lake size which generates higher prediction rates of mixing than squared surface area.

We tested the sensitivity of our stratification predictions using the square root of surface area as a measure of lake size, rather than fetch, in the Gorham-Boyce equations. Under the historical conditions used to generate Supplementary Fig. 11, the number of stratified lakes increased from 14% to 21%. This result points to the value of having reasonable fetch estimates in the Arctic GIS lake database, rather than just estimates of the lake surface area. This is because we want to prevent an overestimation of stratified lakes with potential thermal refugia for coldwater fish species, as this may exaggerate their thermal resources under future climate scenarios.

Regional predictions of the impact of climate change on stratification patterns in Canadian Arctic lakes

We compared projections of future (2050 and 2100) stratification patterns under RCP4.5 and RCP8.5 emission scenarios with patterns based on historical (1986–2005) climate conditions[29]. The fitting procedure outlined in the previous sections demonstrated that, under historical climate conditions, a single Weibull CD percentile value could shape the maximum depth distribution of our lake sample to match the expected distribution derived from semi-mechanistic theory founded on the work of Gorham and Boyce[25] and Hanna[60]. We assumed that this percentile value would be insensitive to the changes associated with future climates and used it to project the impacts of future climate change. The procedure used to project the stratification pattern under each climate change scenario followed that outlined above, except the Weibull CD was fixed at 99.9999 and the climate variables used were extracted from the relevant projected future climate database. Some of the consequences of assuming a fixed CD percentile are outlined below:

(i) an increase in mean summer wind strength will be accompanied by an increase in typical summer storm strength;
(ii) consequently, the percentage of lakes expected to stratify may decline and those lakes that continue to stratify may exhibit deeper thermoclines;
(iii) these directional changes will be opposed if higher wind strengths are accompanied by higher summer surface temperatures, with the overall result determined by the relative strengths of these opposing influences.

Some of these effects are evident in the climate change scenarios that we explored. Specifically, projected storm wind strengths under RCP8.5 are large enough to counter the effects of higher summer water temperatures, leading to deeper projected thermoclines than are evident in both the historical climate simulation and RCP4.5 simulations (Supplementary Tables 16 and 17 and Supplementary Fig. 12).

We summarized these projected changes for each of the terrestrial ecozones that make up the Canadian Arctic region[30]. Several different spatial management divisions have been defined for the Canadian Arctic. We chose to summarize our results by terrestrial ecozones because this system effectively characterizes landscape-level variability in lake morphometry and climate, and it is these variables that underpin our predictions of thermal diversity. We did evaluate an alternative system (freshwater ecoregions[67]) based on partitioning landscape-level variability in fish distributions. However, this partitioning was less effective at capturing landscape variability in either climate or lake characteristics (Supplementary Tables 18–20 and Supplementary Fig. 13) and therefore would not be as useful as ecozones in summarizing landscape-level variability in lake thermal diversity. Changes in thermal diversity will impact all components of these Arctic ecosystems, not just fish communities. Therefore, partitioning based on the drivers of thermal diversity should make our results relevant to a wide range of disciplines. In the Supplementary Material, we compare how these two systems partition landscape-level variation in lake morphometry and

climate (Supplementary Tables 18–20 and Supplementary Fig. 9). We also illustrate (Supplementary Fig. 14) our thermal habitat results by freshwater ecoregion.

Regional predictions of the impact of climate change on fish habitat diversity in Canadian Arctic lakes

North American limnetic fish species can be classified into three thermal guilds (coldwater, coolwater, and warmwater) based on their thermal preferences[68,69]. This classification forms the basis for the three lake types that are the focus of our thermal habitat projections: thermally diverse, thermally uniform, and barren. Thermally diverse lakes have winter ice thicknesses ≤ their mean depth and are stratified while ice-free. These lakes could support native coldwater fish species and provide refuge during summer from coolwater or warmwater invaders. Thermally uniform lakes also have winter ice thicknesses ≤ their mean depth but are fully mixed while ice-free. These lakes would foster competition among native coldwater and invading coolwater or warmwater species because they have no coldwater thermal refuge. Barren lakes have winter ice thicknesses > their mean depth and can be stratified or mixed when ice-free. These lakes are assumed to be incapable of supporting self-sustaining fish populations because they nearly freeze to the bottom in winter. Barren lakes that no longer freeze beyond their mean depth under future climates represent new potential fish habitats. Our climate change projections focus on (i) changes in the relative numbers of these three lake types; and (ii) changes in the supply of suitable habitat for each thermal guild.

The models outlined in previous sections (i.e., ice thickness model, stratification occurrence model) were used to classify individual lakes into our three lake types (barren, thermally uniform, and thermally diverse) under historical and future climates. For lakes deemed to be stratified by the Gorham-Boyce equations, we applied an additional filter to reduce the chance of overestimating the number of stratified lakes. We required the water density difference between its epilimnion and hypolimnion to be 0.5 kg m^{-3}. This corresponds to a thermal difference of 2.52 °C given a hypolimnion temperature of 4 °C.

Projections of suitable thermal habitats for each lake type were based on our definition of thermal guilds. Coker et al.[68] used extant data on the preferred temperature of Canadian freshwater fish to identify three classes or guilds: coldwater—preferred temperature <19 °C; coolwater—preferred temperature [19,25] °C; warmwater—preferred temperature >25 °C. We reviewed the temperature preference data provided in a much more recent compendium for North American freshwater fish[70]. We focused our attention on the 42 species that commonly occur in the Canadian Arctic and concluded that the temperature preference data for these species would be better represented by guild boundaries that were shifted to somewhat lower levels than those presented by Coker et al.[68]. Therefore, in our projections, we used the following thermal guild definitions: coldwater <16 °C, coolwater [16,22] °C, and warmwater >22 °C.

Our lake-specific projections of annual habitat supply for each thermal guild under each climate scenario were determined as follows. Over the ice-free period, we generated daily temperature vs depth profiles for each lake by assuming:

(i) daily lake surface water temperature $[T(j)]$ varies with day j as follows:

$$when\ j \le J_{MAX}\ \&\ j > \mathrm{BU}, T(j) = 4 + \left(\frac{T_{AVG} - T_{HYP}}{(J_{MAX} - \mathrm{BU})^2}\right) \times \left((J_{MAX} - \mathrm{BU})^2 - (j - J_{MAX})^2\right) \quad (13)$$

$$when\ j > J_{MAX}\ \&\ j < \mathrm{FU}, T(j) = 4 + \left(\frac{T_{AVG} - T_{HYP}}{(\mathrm{FU} - J_{MAX})^2}\right) \times \left((\mathrm{FU} - J_{MAX})^2 - (j - J_{MAX})^2\right) \quad (14)$$

Where:

T_{AVG} = average maximum surface water temperature (°C), based on the T_{MAX} model[27] and SWT model[28]

J_{MAX} = date of T_{MAX} (day of year), or the midpoint between the ice break-up and freeze-up dates

BU = ice break-up date (day of year)

FU = ice break-up date (day of year)

T_{HYP} = starting temperature representative of the lake at ice break-up and the hypolimnion during stratification (°C) (if applicable)

(ii) for thermally uniform lakes, the water temperature from the lake surface to its maximum depth on day j is set equal to $T(j)$;

(iii) for thermally diverse lakes, the water temperature from the lake surface to its estimated thermocline depth on day j is set equal to $T(j)$; for depths > the estimated thermocline depth, the temperature is set equal to 4 °C.

We calculated the annual habitat supply for each thermal guild as follows. We began by characterizing the shape of the lake basin. We assumed that the basin was cone-shaped and used the known surface area and maximum depth of each lake to generate a value for the dimensionless volume development (V_d) parameter. V_d describes the lake basin shape in relation to the volume of a cone with a base area and height equal to the lake's surface area and maximum depth[71]:

$$V_d = \frac{\text{mean depth}}{\text{maximum depth}} \quad (15)$$

We then used this parameter in the R package 'rLakeAnalyzer' and its *approx.bathy* function to divide the total lake volume into successive 0.1 m layers starting at the surface and extending to the bottom of the lake[72]. This package was not used in the estimation of mean and maximum lake depth for the dataset. This permitted us to easily estimate the total lake volume for thermally uniform lakes and the lake volumes above and below the thermocline for thermally diverse lakes (as well as stratified and unstratified barren lakes). We then calculated the annual habitat supply for fish belonging to each thermal guild as follows:

coldwater guild volume-days (CdVD, m^3 days):

$$\sum_{j=\mathrm{BU}}^{j=\mathrm{FU}} V(j)_{<16} \quad (16)$$

coolwater guild volume-days (ClVD, m^3 days):

$$\sum_{j=\mathrm{BU}}^{j=\mathrm{FU}} V(j)_{[16,22]} \quad (17)$$

warmwater guild volume-days (WVD, m^3 days):

$$\sum_{j=\mathrm{BU}}^{j=\mathrm{FU}} V(j)_{[>22]} \quad (18)$$

Where:

$V(j)_{<16}$ = lake volume on day j that has a temperature <16 °C

$V(j)_{[16,22]}$ = lake volume on day j that has a temperature in the interval [16,22] °C

$V(j)_{>22}$ = lake volume on day j that has a temperature >22 °C

We did not attempt to estimate seasonal hypolimnion dynamics in stratified lakes. We assumed that hypolimnetic water would be sufficiently cold to serve as a refuge for coldwater fish species. This assumption is consistent with the range of hypolimnetic temperatures generated using the

lake layer density difference model for the historical period (range = 4.00–11.62 °C, mean = 8.45 °C).

Lakes with small, fleeting thermally suitable fish habitats may not have sufficient thermal resources for fish to establish viable populations. For example, if a lake epilimnion reaches 16–17 °C for a few days this could be considered coolwater thermal habitat; however, it is unlikely that this small, transient thermal habitat would be sufficient for a coolwater fish population to establish. We set establishment thresholds for coolwater and warmwater fish thermal habitats to prevent including lakes where these temperatures only appear briefly. We based these thresholds on earlier research that linked the northern range limits of typical members of these guilds (yellow perch *Perca flavescens* and smallmouth bass *Micropterus dolomieu*, respectively) to the severity of winter starvation[42], as indexed by mean annual air temperature[28,42,73]. Mean annual air temperatures of −1.8 °C marked the northern distributional limit for yellow perch in North America, and +1.9 °C marked the northern limit for smallmouth bass. In both species, these values for air temperature were associated with annual water temperature regimes that supported low levels of reproductive success due to short growing seasons and consequent long periods of winter starvation[72]. Given this association between the boundary marking population viability (the northern distributional limit) and specific air temperatures, we assumed that the maximum surface water temperature associated with these air temperatures could be used as establishment thresholds for coolwater and warmwater fish populations. Following the approach used in this earlier analysis, we used the empirical model of Shuter et al.[74] to estimate these maximum surface water temperatures as follows:

$$\ln \mathrm{AP} = 3.059 + 0.0422 \times T_{\mathrm{ANN}} - 0.002 \times {T_{\mathrm{ANN}}}^2 \times \ln \mathrm{TORZ}^3 \quad (19)$$

Where:
ln AP = the natural logarithm of maximum surface water temperature (°C)
T_{ANN} = mean annual air temperature (°C)
ln TORZ = thermally diverse lakes: the natural logarithm of thermocline depth (m); thermally uniform lakes: the natural logarithm of mean depth (m)

We calculated ln AP for all thermally diverse and thermally uniform lakes under the historical climate scenario (barren lakes were excluded because they are assumed to have no fish habitat). We then calculated the mean of the AP estimates for all thermal habitat lakes (i.e., thermally diverse, and thermally uniform lakes), resulting in a peak surface water temperature of 19.32 °C at −1.8 °C mean annual air temperature (coolwater establishment threshold), and 22.54 °C at 1.9 °C mean annual air temperature (warmwater establishment threshold). We rounded the coolwater threshold down to 19 °C to be closer to the yellow perch final temperature preferendum (17.6 °C) and rounded the warmwater fish establishment threshold up to 23 °C to be closer to the smallmouth bass final temperature preferendum (25 °C). The final temperature preferendum is the temperature that a fish will gravitate towards when exposed to a thermal gradient, regardless of its acclimation history[74].

We also developed a persistence time threshold for coldwater fish to be applied to unstratified lakes. This prevented the inclusion of lakes, in our thermal habitat summary, where the entire water column temperature exceeds the upper thermal limit for coldwater fish for extended periods. We based this threshold on the mean upper incipient lethal temperature for coldwater Arctic fish species[70], which is 24.07 °C (n species = 18) rounded down to 24 °C for 14 days or greater. This number of days aligns with field-based estimates of thermal tolerance for coldwater trout species[75].

We only report thermal habitat metrics for lakes that meet the establishment/persistence criteria described above. For example, the warmwater volume-days from a lake that has a peak surface temperature of 22.5 °C would not be included in our cumulative total of warmwater fish habitat because the establishment threshold of 23 °C is not reached in that lake. We calculated indices of the relative amount of thermal habitat available for each thermal guild (Fig. 7) as follows:

relative amount of coldwater thermal habitat:

$$100 \times \frac{\mathrm{CdVD}}{\mathrm{CdVD} + \mathrm{ClVD} + \mathrm{WVD}} \quad (20)$$

relative amount of coldwater thermal habitat:

$$100 \times \frac{\mathrm{ClVD}}{\mathrm{CdVD} + \mathrm{ClVD} + \mathrm{WVD}} \quad (21)$$

relative amount of warmwater thermal habitat:

$$100 \times \frac{\mathrm{WVD}}{\mathrm{CdVD} + \mathrm{ClVD} + \mathrm{WVD}} \quad (22)$$

We conducted all data transformation and analyses in the R statistical environment (R version 4.2.0)[76].

See Supplementary Figs. 15–32 for maps showing projected changes in all metrics presented in this study summarized as regional averages represented by 0.5° grid cells.

Data availability

Data for this study is available on Dryad: https://doi.org/10.5061/dryad.cvdncjt8g.

Code availability

The code used to conduct the analysis for this study is forthcoming on *Zenodo*, and will be accessible through Dryad: https://doi.org/10.5061/dryad.cvdncjt8g.

Received: 14 August 2023; Accepted: 31 January 2024;
Published online: 20 February 2024

References

1. IPCC. Climate change 2014: impacts, adaptation and vulnerability. in *Summary for Policy Makers* (eds. Field, C. et al.) 1–32 (Cambridge University Press, 2014).
2. Box, J. E. et al. Key indicators of Arctic climate change: 1971–2017. *Environ. Res. Lett.* **14**, 045010 (2019).
3. Holland, M. M. & Bitz, C. M. Polar amplification of climate change in coupled models. *Clim. Dyn.* **21**, 221–232 (2003).
4. Adrian, R. et al. Lakes as sentinels of climate change. *Limnol. Oceanogr.* **54**, 2283–2297 (2009).
5. Douglas, M. S. V., Smol, J. P. & Blake, W. Marked post-18th century environmental change in high-arctic ecosystems. *Science (80-.)* **266**, 416–419 (1994).
6. Rühland, K., Priesnitz, A. & Smol, J. P. Paleolimnological evidence from diatoms for recent environmental changes in 50 lakes across Canadian arctic treeline. *Arctic Antarct. Alp. Res.* **35**, 110–123 (2003).
7. Kraemer, B. M. et al. Morphometry and average temperature affect lake stratification responses to climate change. *Geophys. Res. Lett.* **42**, 4981–4988 (2015).
8. Lopez, L. S., Hewitt, B. A. & Sharma, S. Reaching a breaking point: how is climate change influencing the timing of ice breakup in lakes across the northern hemisphere? *Limnol. Oceanogr.* **64**, 2621–2631 (2019).
9. Hewitt, B. A. et al. Historical trends, drivers, and future projections of ice phenology in small north temperate lakes in the Laurentian Great Lakes Region. *Water (Switzerland)* **10**, 70 (2018).
10. Shuter, B. J., Minns, C. K. & Fung, S. R. Empirical models for forecasting changes in the phenology of ice cover for Canadian lakes. *Can. J. Fish. Aquat. Sci.* **70**, 982–991 (2013).

11. Dibike, Y., Prowse, T., Bonsal, B., Rham, Lde & Saloranta, T. Simulation of North American lake-ice cover characteristics under contemporary and future climate conditions. *Int. J. Climatol.* **32**, 695–709 (2012).
12. Sommaruga-Wögrath, S. et al. Temperature effects on the acidity of remote alpine lakes. *Nature* **387**, 64–67 (1997).
13. Campana, S. E. et al. Arctic freshwater fish productivity and colonization increase with climate warming. *Nat. Clim. Chang.* **10**, 428–433 (2020).
14. King, J. R., Shuter, B. J. & Zimmerman, A. P. Empirical links between thermal habitat, fish growth, and climate change. *Trans. Am. Fish. Soc.* **128**, 656–665 (1999).
15. Sorvari, S., Korhola, A. & Thompson, R. Lake diatom response to recent Arctic warming in Finnish Lapland. *Glob. Chang. Biol.* **8**, 171–181 (2002).
16. Woolway, R. I., Sharma, S. & Smol, J. P. Lakes in hot water: the impacts of a changing climate on aquatic ecosystems. *Bioscience* **72**, 1050–1061 (2022).
17. Christie, G. C. & Regier, H. A. Measures of optimal thermal habitat and their relationship to yields of four commercial fish species. *Can. J. Fish. Aquat. Sci.* **45**, 301–314 (1988).
18. Arctic Climate Impact Assessment. *Impacts of a Warming Arctic—Arctic Climate Impact Assessment*. (Cambridge University Press, 2004).
19. Galappaththi, E. K., Ford, J. D., Bennett, E. M. & Berkes, F. Climate change and community fisheries in the Arctic: a case study from Pangnirtung, Canada. *J. Environ. Manag.* **250**, 109534 (2019).
20. Reist, J. D. et al. An overview of effects of climate change on selected Arctic freshwater and Anadromous fishes. *Ambio* **35**, 381–387 (2006).
21. Jacobson, P. C., Cross, T. K., Zandlo, J., Carlson, B. N. & Pereira, D. P. The effects of climate change and eutrophication on cisco *Coregonus artedi* abundance in Minnesota lakes. *Adv. Limnol.* **63**, 417–427 (2012).
22. Haynes, T. B., Rosenberger, A. E., Lindberg, M. S., Whitman, M. & Schmutz, J. A. Patterns of lake occupancy by fish indicate different adaptations to life in a harsh Arctic environment. *Freshw. Biol.* **59**, 1884–1896 (2014).
23. Hulsman, M. F. et al. Influence of potential fish competitors on Lake Trout trophic ecology in small lakes of the Barrenlands, N.W.T. *Canada. J. Great Lakes Res.* **42**, 290–298 (2016).
24. McMeans, B. C. et al. Winter in water: differential responses and the maintenance of biodiversity. *Ecol. Lett.* **23**, 922–938 (2020).
25. Gorham, E. & Boyce, F. M. Influence of lake surface area and depth upon thermal stratification and the depth of the summer thermocline. *J. Great Lakes Res.* **15**, 233–245 (1989).
26. Minns, C. K. & Shuter, B. J. A semi-mechanistic seasonal temperature-profile model (STM) for the period of stratification in dimictic lakes. *Can. J. Fish. Aquat. Sci.* **70**, 169–181 (2013).
27. Gillis, D. P., Minns, C. K. & Shuter, B. J. Predicting open-water thermal regimes of temperate North American lakes. *Can. J. Fish. Aquat. Sci*. **78**, 820–840 (2021).
28. Sharma, S., Jackson, D. A., Minns, C. K. & Shuter, B. J. Will northern fish populations be in hot water because of climate change? *Glob. Chang. Biol*. **13**, 2052–2064 (2007).
29. Government of Canada. *Climate Data Extraction Tool*. https://climate-change.canada.ca/climate-data/#/ (Government of Canada, 2021).
30. Ricketts, T. A. et al. *Terrestrial Ecoregions of North America—A conservation assessment*. (Island Press Books, 1999).
31. Saros, J. E. et al. Sentinel responses of Arctic freshwater systems to climate: linkages, evidence, and a roadmap for future research. *Arct. Sci.* **37**, 1–37 (2022).
32. Grant, L. et al. Attribution of global lake systems change to anthropogenic forcing. *Nat. Geosci.* **14**, 849–854 (2021).
33. O'Reilly, C. M. et al. Rapid and highly variable warming of lake surface waters around the globe. *Geophys. Res. Lett.* **42**, 10773–10781 (2015).
34. Myers, B. J. E. et al. Global synthesis of the documented and projected effects of climate change on inland fishes. *Rev. Fish Biol. Fish.* **27**, 339–361 (2017).
35. Van Zuiden, T. M., Chen, M. M., Stefanoff, S., Lopez, L. & Sharma, S. Projected impacts of climate change on three freshwater fishes and potential novel competitive interactions. *Divers. Distrib.* **22**, 603–614 (2016).
36. Roux, M. J., Tallman, R. F. & Lewis, C. W. Small-scale Arctic charr Salvelinus alpinus fisheries in Canada's Nunavut: management challenges and options. *J. Fish Biol.* **79**, 1625–1647 (2011).
37. Grenier, G. & Tallman, R. F. Lifelong divergence of growth patterns in Arctic charr life history strategies: implications for sustainable fisheries in a changing climate. *Arct. Sci.* **7**, 454–470 (2021).
38. Laske, S. M. et al. Surface water connectivity drives richness and composition of Arctic lake fish assemblages. *Freshw. Biol.* **61**, 1090–1104 (2016).
39. Samarasin, P., Minns, C. K., Shuter, B. J., Tonn, W. M. & Rennie, M. D. Fish diversity and biomass in northern Canadian lakes: Northern lakes are more diverse and have greater biomass than expected based on species–energy theory. *Can. J. Fish. Aquat. Sci.* **72**, 226–237 (2014).
40. Rypel, A. L. & David, S. R. Pattern and scale in latitude-production relationships for freshwater fishes. *Ecosphere* **8**, e01660 (2017).
41. Hansen, G. J. A., Wehrly, K. E., Vitense, K., Walsh, J. R. & Jacobson, P. C. Quantifying the resilience of coldwater lake habitat to climate and land use change to prioritize watershed conservation. *Ecosphere* **13**, 1–18 (2022).
42. Shuter, B. J. & Post, J. R. Climate, population viability, and the zoogeography of temperate fishes. *Trans. Am. Fish. Soc.* **119**, 314–336 (1990).
43. Eloranta, A. P., Nieminen, P. & Kahilainen, K. K. Trophic interactions between introduced lake trout (*Salvelinus namaycush*) and native Arctic charr (*S. alpinus*) in a large Fennoscandian subarctic lake. *Ecol. Freshw. Fish* **24**, 181–192 (2015).
44. Rolls, R. J., Hayden, B. & Kahilainen, K. K. Conceptualising the interactive effects of climate change and biological invasions on subarctic freshwater fish. *Ecol. Evol.* **7**, 4109–4128 (2017).
45. Vasseur, D. A. et al. Increased temperature variation poses a greater risk to species than climate warming. *Proc. R. Soc. B Biol. Sci*. **281**, 20132612 (2014).
46. Reist, J. D. et al. General effects of climate change on arctic fishes and fish populations. *Ambio* **35**, 370–380 (2006).
47. Meinshausen, M. et al. The RCP greenhouse gas concentrations and their extensions from 1765 to 2300. *Clim. Change* **109**, 213–241 (2011).
48. Amante, C. & Eakins, B. W. ETOP01 arc-minute global relief model: procedures, data sources and analysis. NOAA Technical Memorandum NESDIS NGDC-24. https://doi.org/10.7289/V5C8276M (2009).
49. Bird, R. E. & Hulstrom, R. L. *A Simplified Clear Sky Model for Direct and Diffuse Insolation on Horizontal Surfaces*. https://doi.org/10.2172/6510849 (Solar Energy Research Institute, 1981).
50. Kasten, F. & Czeplak, G. Solar and terrestrial radiation dependent on the amount and type of cloud. *Sol. Energy* **24**, 177–189 (1980).
51. Harris, I., Jones, P. D., Osborn, T. J. & Lister, D. H. Updated high-resolution grids of monthly climatic observations—the CRU TS3.10 Dataset. *Int. J. Climatol.* **34**, 623–642 (2014).
52. Murdoch, A. et al. Drivers of fish biodiversity in a rapidly changing permafrost landscape. *Freshw. Biol.* **66**, 2301–2321 (2021).
53. Minns, C. K., Moore, J. E., Shuter, B. J. & Mandrak, N. E. A preliminary national analysis of some key characteristics of Canadian lakes. *Can. J. Fish. Aquat. Sci.* **65**, 1763–1778 (2008).

54. Messager, M. L., Lehner, B., Grill, G., Nedeva, I. & Schmitt, O. Estimating the volume and age of water stored in global lakes using a geo-statistical approach. *Nat. Commun.* **7**, 13603 (2016).
55. Minns, C. K., Shuter, B. J. & Fung, S. *Regional projections of climate change effects on ice cover and open-water duration for Ontario lakes using updated ice-date models. Climate Change Research Report CCRR-40*. (Ontario Forest Research Institute, Ontario Ministry of Natural Resources, 2014).
56. Read, J. S. et al. Simulating 2368 temperate lakes reveals weak coherence in stratification phenology. *Ecol. Modell.* **291**, 142–150 (2014).
57. Read, J. S. et al. Process-guided deep learning predictions of lake water temperature. *Water Resour. Res.* **55**, 9173–9190 (2019).
58. Yang, B. et al. A new thermal categorization of ice-covered lakes. *Geophys. Res. Lett.* **48**, e2020GL091374 (2021).
59. Straskraba, M. The effects of physical variables on freshwater production: analyses based on models. In *The functioning of freshwater ecosystems* (eds. Le Cren, E. D. & Lowe-McConnell, R. H.) 13–84 (Cambridge University Press, 1980).
60. Hanna, M. Evaluation of models predicting mixing depth. *Can. J. Fish. Aquat. Sci.* **47**, 940–947 (1990).
61. Wüest, A. & Lorke, A. Small-scale hydrodynamics in lakes. *Annu. Rev. Fluid Mech.* **35**, 373–412 (2003).
62. Hsu, S. A., Meindl, E. A. & Gilhousen, D. B. Determining the power-law wind-profile exponent under near-neutral stability conditions at sea. *J. Appl. Meteorol.* **33**, 757–765 (1994).
63. Conradsen, K., Nielsen, L. B. & Prahm, L. P. Review of Weibull statistics for estimation of wind speed. *Distributions. J. Clim. Appl. Meteorol.* **23**, 1173–1183 (1984).
64. Wickham, H., Francois, R., Henry, L. & Müller, K. dplyr: A grammar of data manipulation. R package version 1.0.9 (2022).
65. Charnock, H. Wind stress on a water surface. *Quarterly Journal of the Royal Meteorological Society* **81**, 639–640 (1955).
66. Boyce, F. M., Moody, W. J. & Killins, B. L. *Heat Content of Lake Ontario and Estimates of Average Surface Heat Fluxes During IFYGL*. (Fisheries and Environment Canada, Inland Waters Directorate, Canada Centre for Inland Waters, 1977).
67. Abell, R. et al. Freshwater ecoregions of the world: a new map of biogeographic units for freshwater biodiversity conservation. *Bioscience* **58**, 403–414 (2008).
68. Coker, G. A., Portt, C. B. & Minns, C. K. Morphological and ecological characteristics of Canadian freshwater fishes. *Canadian Manuscript Report of Fisheries and Aquatic Sciences*. 2554 http://publications.gc.ca/collections/collection_2007/dfo-mpo/Fs97-4-2554E.pdf (Fisheries and Oceans Canada, 2001).
69. Magnuson, J. J., Crowder, L. B. & Medvick, P. A. Temperature as an ecological resource. *Am. Zool.* **19**, 331–343 (1979).
70. Hasnain, S. S., Escobar, M. D. & Shuter, B. J. Estimating thermal response metrics for North American freshwater fish using Bayesian phylogenetic regression. *Can. J. Fish. Aquat. Sci.* **75**, 1878–1885 (2018).
71. Johansson, H., Brolin, A. A. & Håkanson, L. New approaches to the modelling of lake basin morphometry. *Environ. Model. Assess.* **12**, 213–228 (2007).
72. Winslow, L. et al. rLakeAnalyzer: Lake physics tools. R package version 1.11.4.1 (2019).
73. Shuter, B. J., Schlesinger, D. A. A. & Zimmerman, A. P. P. Empirical predictors of annual surface water temperature cycles in North American lakes. *Can. J. Fish. Aquat. Sci.* **40**, 1838–1845 (1983).
74. Fry, F. E. J. *Effects of the Environment on Animal Activity.* No. 68 (Publications of the Ontario Fisheries Research Laboratory, 1947).
75. Wehrly, K. E., Wang, L. & Mitro, M. Field-based estimates of thermal tolerance limits for trout: incorporating exposure time and temperature fluctuation. *Trans. Am. Fish. Soc.***136**, 365–374 (2007).
76. R Core Team. R: A language and environment for statistical computing. R Foundation for Statistical Computing (2022).

Acknowledgements

This work was supported by grants from the Canadian Network for Aquatic Ecosystems Services and the Discovery Grant program of the Natural Sciences and Engineering Research Council of Canada. We thank Gerald Black for his crucial role in developing the Arctic Lake database. His work was supported by the Nunavut Wildlife Management Board, Fisheries and Oceans Canada, US National Science Foundation grant OCE-9985884, and the University of Iceland. We are grateful for the efforts made by those who conducted or collaborated with the various field programs that generated the data used and cited in our study. We thank Alyssa Murdoch for providing lake data for our lake morphometry ground-truthing and for helpful comments on an earlier draft of the paper. We thank Mathew Wells for the helpful discussions and guidance during the formative stages of the paper. Additional support from Don Jackson and the University of Toronto is much appreciated. Comments and suggestions from two anonymous reviewers inspired extensive changes that greatly improved the quality of the manuscript.

Author contributions

D.P.G. conceived, designed, and refined the project, performed most of the analysis and modeling, interpreted the results, and wrote the manuscript. C.K.M. interpreted the results and contributed to the manuscript writing. S.E.C. provided the lake morphometry database and helped integrate it into the overall analysis, interpreted the results, and contributed to the manuscript writing. B.J.S. conceived, designed, and refined the project, provided ideas and supporting analyses for the stratification modeling, interpreted the results, and contributed to the manuscript writing.

Competing interests

The authors declare no competing interests.

Additional information

Supplementary information The online version contains supplementary material available at https://doi.org/10.1038/s43247-024-01251-8.

Correspondence and requests for materials should be addressed to Daniel P. Gillis.

Peer review information *Communications Earth & Environment* thanks the anonymous reviewers for their contribution to the peer review of this work. Primary handling editors: Michael Stukel and Clare Davis. A peer review file is available.